

# PHOTOREDOX CATALYSIS BY $[\text{Ru}(\text{bpy})_3]^{2+}$ TO TRIGGER TRANSFORMATIONS OF ORGANIC MOLECULES. ORGANIC SYNTHESIS USING VISIBLE-LIGHT PHOTOCATALYSIS AND ITS 20th CENTURY ROOTS

Filip TEPLÝ

*Institute of Organic Chemistry and Biochemistry, Academy of Sciences of the Czech Republic, v.v.i., Flemingovo nám. 2, 166 10 Prague 6, Czech Republic; e-mail: teply@uochb.cas.cz*

Received April 17, 2011

Accepted June 10, 2011

Published online June 29, 2011

*Dedicated to Professor Pavel Kočovský on the occasion of his 60th birthday.*

1. Introduction . . . . .	860
2. Photoredox Manifold of $[\text{Ru}(\text{bpy})_3]^{2+}$ . . . . .	860
3. Early Examples from the 1970s to 1990s . . . . .	862
4. Photoredox Catalysis in the First Decade of the 21st Century. . . . .	880
5. Photoredox Chemistry as a Tool for Making and Breaking Bonds in Chemical Biology and Materials Chemistry. . . . .	905
5.1. Chemical Biology . . . . .	905
5.2. Materials Chemistry . . . . .	907
6. Conclusions and Outlook . . . . .	911
7. Abbreviations . . . . .	912
8. References and Notes . . . . .	913

Reactions triggered by light constitute a treasure trove of unique synthetic methods that are available to chemists. Photoinduced redox processes using visible light in conjunction with sensitizing dyes offer a great variety of catalytic transformations useful in the realm of organic synthesis. The recent literature amply shows that this preparative toolbox is expanding substantially. This review discusses historical and contemporary work in the area of photoredox catalysis with  $[\text{Ru}(\text{bpy})_3]^{2+}$ . Elegant examples from the most recent literature document the importance of this fast developing area of research. The photoredox chemistry has also emerged as a promising bond-making and bond-breaking tool for chemical biology and materials chemistry. A review with 96 references.

**Keywords:** Ruthenium complexes; Catalysis with dyes; Photocatalysis; Photoredox catalysis;  $[\text{Ru}(\text{bpy})_3]^{2+}$ ; Visible light; Organic synthesis; Chemical biology; Materials chemistry; Synthetic methods.

## 1. INTRODUCTION

Transformations induced by light have been attracting attention of chemists since the early 20th century<sup>1–3</sup>. Among various photochemical reactions, photoredox catalysis using combination of  $[\text{Ru}(\text{bpy})_3]^{2+}$  catalyst and visible light has been considered as a tool for preparative organic chemistry since the 1970s. However, only a few research groups dealt with this topic until the beginning of the 21st century. Remarkably, since 2008, the importance of this bond-forming strategy for organic synthesis has been dramatically highlighted due to the seminal studies by MacMillan, Yoon, and Stephenson groups<sup>4–7</sup>. With this rejuvenated interest in organic transformations triggered by metal-based dyes, and very recently also purely organic dyes<sup>8</sup>, as photoredox catalysts, it is interesting to look for the 20th century roots of this branch of research. In this review we will focus on the pioneering examples from the 20th century as well as elegant examples from the most recent literature to document the significance of this fast developing area of research. Throughout the review the emphasis will be placed mainly on  $[\text{Ru}(\text{bpy})_3]^{2+}$  (Fig. 1) and the transformations where this complex has been used as a photoredox catalyst.

## 2. PHOTOREDOX MANIFOLD OF $[\text{Ru}(\text{bpy})_3]^{2+}$

Salts of  $[\text{Ru}(\text{bpy})_3]^{2+}$  (**1**, bpy = 2,2'-bipyridine) were first reported by Burstall in 1936 (Fig. 1)<sup>9</sup>. Notably, Burstall also achieved resolution of the two enantiomers of **1** via diastereomeric tartrate salts<sup>9</sup>. At that time, it was shown that  $[\text{Ru}(\text{bpy})_3]^{2+}$  was not only chemically robust, but also remarkably configurationally stable species<sup>10</sup>. Whereas chirality of this  $C_3$ -symmetric complex cation has been recognized at the time of its first synthesis, its unique photochemical and electrochemical properties have attracted attention with a more than 30-year delay<sup>11,12</sup>. However, then the research focused on photoredox manifold of  $[\text{Ru}(\text{bpy})_3]^{2+}$  and its applications has experienced a massive expansion and especially the conversion of solar radiation into other forms of energy has been studied vigorously. In particular, conversion of solar energy into electrical current<sup>13</sup> and into chemical energy of fuels by photoreduction of small molecules, such as water and  $\text{CO}_2$ , have received focused attention due to the practical implications of harnessing solar energy to meet the global energy needs<sup>14</sup>. Besides this, even in the beginning of the 21st century,  $[\text{Ru}(\text{bpy})_3]^{2+}$  and its rich spectrum of useful properties continues to inspire important conceptual advances in other areas, as recently discussed by Balzani et al. in the context of a novel molecular encoder–decoder for sensing, labeling, or molecular computing<sup>15</sup>.

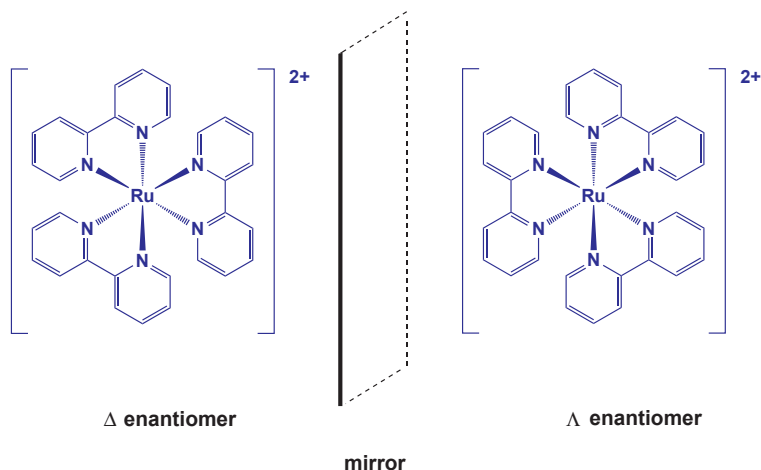
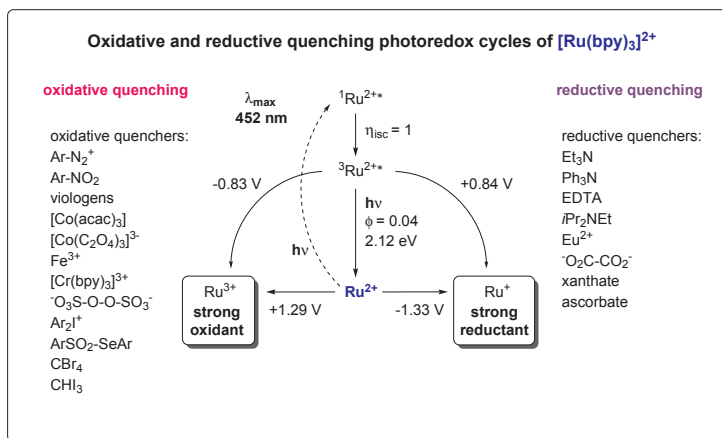


FIG. 1  
Structure of  $[\text{Ru}(\text{bpy})_3]^{2+}$  (1) and its chirality

Visible light matches well a broad absorption band of  $[\text{Ru}(\text{bpy})_3]^{2+}$  complex ( $\lambda_{\text{max}} = 452 \text{ nm}$ ) leading to efficient excitation that gives the lowest singlet excited state ( $^1\text{Ru}^{2+*}$  in Scheme 1). This initially generated singlet state ( $^1\text{MLCT}$  state, MLCT = metal-to-ligand charge transfer) then undergoes intersystem crossing yielding a long-lived luminescent triplet excited state  $[\text{Ru}(\text{bpy})_3]^{2+*}$  ( $^3\text{MLCT}$ ,  $^3\text{Ru}^{2+*}$  in Scheme 1). The triplet excited state is gen-

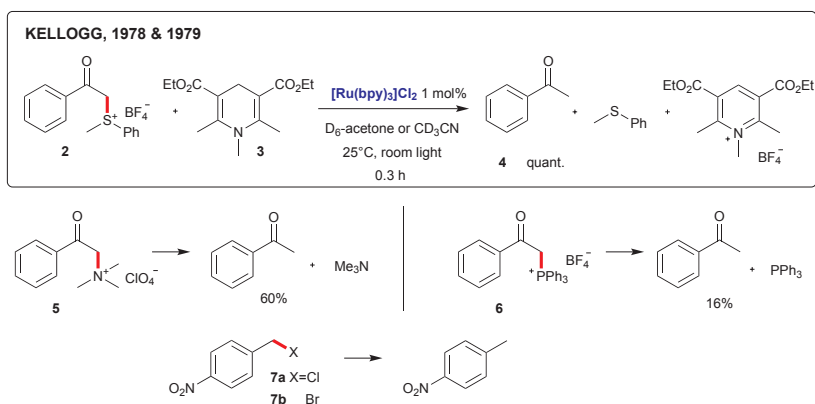


SCHEME 1  
Photoredox manifold of  $[\text{Ru}(\text{bpy})_3]^{2+}$  and representative oxidative and reductive quenchers

erated with highest quantum efficiency and is long-lived (~600 ns). This high energy species can serve either as a single-electron oxidant or reductant depending on other chemical species present. If reductive quenching of the  $[\text{Ru}(\text{bpy})_3]^{2+}$  takes place, strongly reducing species  $[\text{Ru}(\text{bpy})_3]^+$  is produced (-1.33 V vs SCE in  $\text{CH}_3\text{CN}$ ), whereas oxidative quenching pathway generates  $[\text{Ru}(\text{bpy})_3]^{3+}$  that is a strong oxidant (+1.29 V vs SCE in  $\text{CH}_3\text{CN}$ ). Depending on the choice of suitable reductive or oxidative quencher, the  $[\text{Ru}(\text{bpy})_3]^{2+}$  catalyst can be used to trigger photo-reduction and photooxidation, respectively (Scheme 1). As the recent literature shows, this photoredox manifold offers unique opportunities how visible light can be channeled to trigger formation of chemical bonds that are of interest for preparative organic chemistry<sup>4</sup>.

### 3. EARLY EXAMPLES FROM THE 1970s TO 1990s

In 1978, Kellogg's group reported reduction of phenacylsulphonium salts (e.g. **2**) by 1,4-dihydropyridine **3** ( $2 + 3 \rightarrow 4$ , Scheme 2). The reaction was found to be induced by irradiation with visible light and greatly accelerated in the presence of  $[\text{Ru}(\text{bpy})_3]^{2+}$  and other dyes, such as TPP (meso-tetraphenylporphine), or eosin disodium salt<sup>16</sup>. Importantly, the roles of light and dyes were carefully tested. Thus, a control reaction performed in the dark in an absence of sensitizing dye did not lead to any conversion at room temperature even after 72 h. However, the reaction reached complete conversion upon exposure of the same reaction mixture to incident room light for 48 h (neon fluorescent lamps at ca. 2 m distance). Addition of

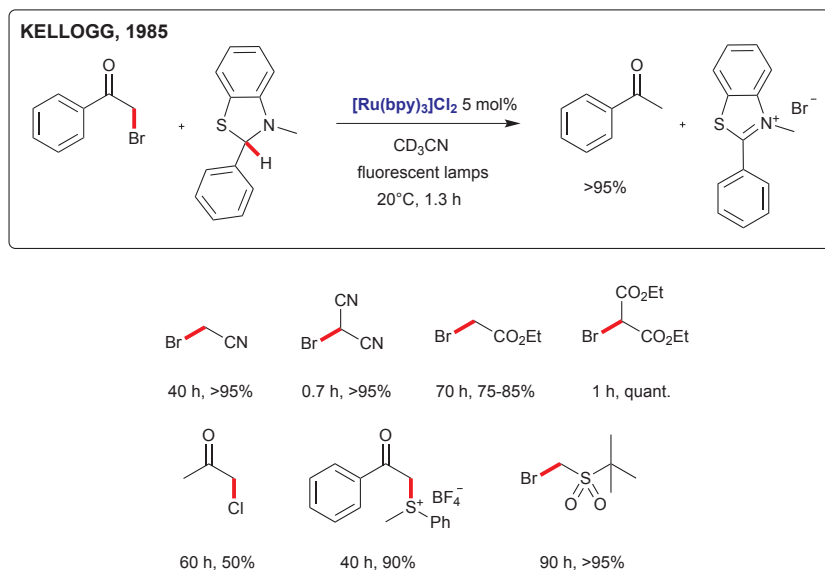


SCHEME 2

Dye-accelerated photoreduction of phenacyl sulfonium salt **2** and related substrates (refs<sup>16,17</sup>)

1 mole % of  $[\text{Ru}(\text{bpy})_3]\text{Cl}_2$ , TPP, or eosin disodium salt led to acceleration of the irradiated reactions resulting in complete conversions within significantly shorter reaction times of 0.3, 1 and 3 h, for the three dyes, respectively. The authors suggested that light-induced single-electron transfer steps are responsible for the observed sulfonium salt reduction and proposed that the large acceleration effect of  $[\text{Ru}(\text{bpy})_3]\text{Cl}_2$  might be due to the involvement of this photoredox catalyst in the single-electron transfers (SET)<sup>16</sup>. Later on, results of a more detailed mechanistic study were disclosed<sup>17</sup>. Although the authors did not arrive at a definitive conclusion about the exact role of  $[\text{Ru}(\text{bpy})_3]^{2+}$  in this process, an impressively insightful discussion of the gathered body of evidence was presented<sup>17</sup>.

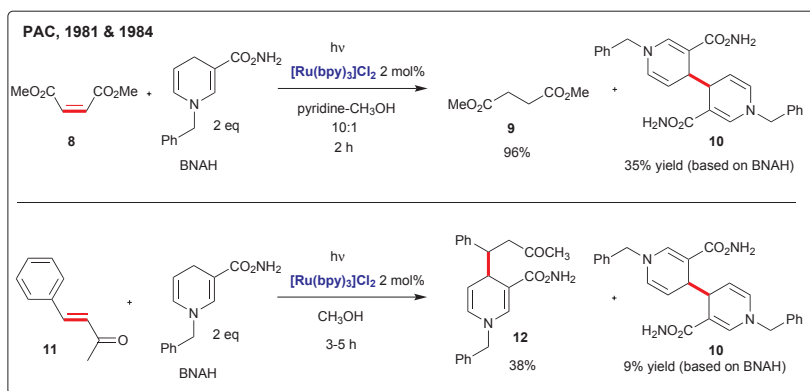
Reductions of other substrates such as ammonium, phosphonium salts, and 4-nitrobenzyl halides have been also achieved (**5**, **6**, **7a** and **7b**, respectively, Scheme 2)<sup>16,17</sup>. In 1985, the same group described reductions of phenacylbromide, bromomalonates, and related substrates (Scheme 3) using 3-methyl-2,3-dihydrobenzothiazoles using  $[\text{Ru}(\text{bpy})_3]\text{Cl}_2$  or rose bengal as photocatalysts<sup>18</sup>. All these examples provided important early evidence that various dyes can function as remarkable accelerators of some light-induced reductions.



SCHEME 3

Dye-enhanced photoreductions at saturated carbon atoms using 3-methyl-2,3-dihydrobenzothiazole reductant (ref.<sup>18</sup>)

Another type of transformations photosensitized by  $[\text{Ru}(\text{bpy})_3]^{2+}$  have been independently discovered by the group of Pac (Scheme 4)<sup>19,20</sup>. In their work, Pac et al. studied reactions of various olefins with 1-benzyl-1,4-dihydronicotinamide (BNAH) as an NADH model. The outcome of these processes were shown to be substrate specific. For example, dimethyl maleate **8** afforded mainly dimethyl succinate (**9**), whereas olefin **11** led to a product **12** containing dihydropyridine moiety.

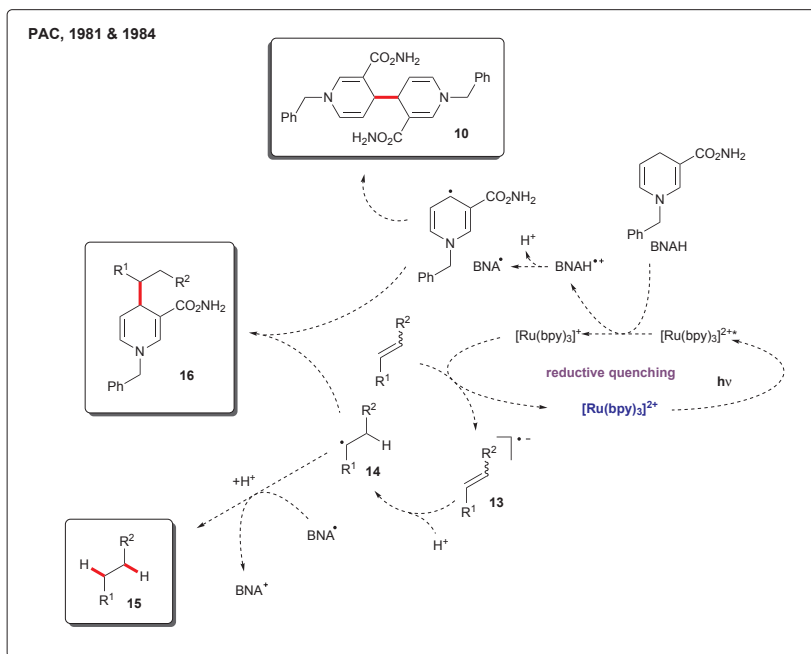


SCHEME 4

$[\text{Ru}(\text{bpy})_3]^{2+}$ -catalyzed photoreduction of olefins with 1-benzyl-1,4-dihydronicotinamide (refs<sup>19,20</sup>)

To account for the observed results, the authors provided a mechanistic rationale depicted in Scheme 5. Ruthenium catalyst was proposed to participate in this transformation via reductive quenching cycle. To this end, the photocatalyst excited state  $[\text{Ru}(\text{bpy})_3]^{2+*}$  is reductively quenched by BNAH to form in situ  $[\text{Ru}(\text{bpy})_3]^+$  and  $\text{BNAH}^{*+}$ . The latter species can subsequently lose proton leading to  $\text{BNA}^*$  that will result in production of the dimer **10**. Strongly reducing  $[\text{Ru}(\text{bpy})_3]^+$  was proposed to transfer its electron onto the olefin substrate to generate the radical anion **13** that is then protonated to give radical intermediate **14**. The resultant radical **14** can be either reduced to the product **15** or can alternatively lead to the structure **16** containing dihydropyridine moiety. Whether radical **14** undergoes electron transfer resulting in structure **15** or leads to radical-coupling giving dihydropyridine product **16**, depends on steric and electronic properties of **14** that should be affected by the substituents at the radical center.

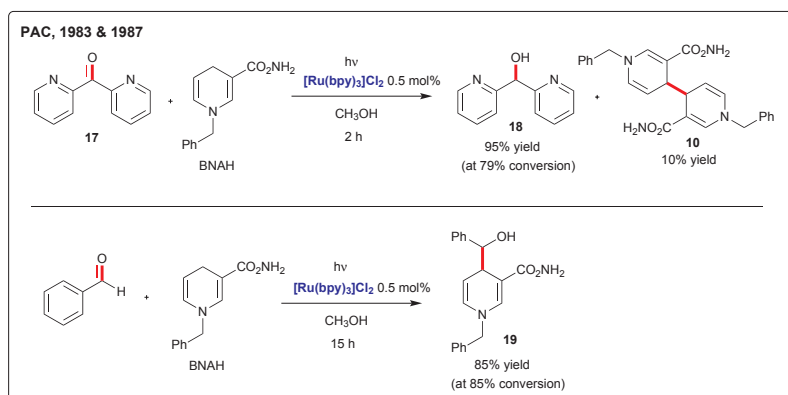
In a related work, Pac and coworkers disclosed reactivity of aromatic carbonyl compounds with BNAH under similar conditions (Scheme 6)<sup>21,22</sup>. The reaction course was found to be governed by the structural parameters



SCHEME 5

Mechanistic picture proposed for the transformations of olefins in Scheme 4 (refs.<sup>19,20</sup>)

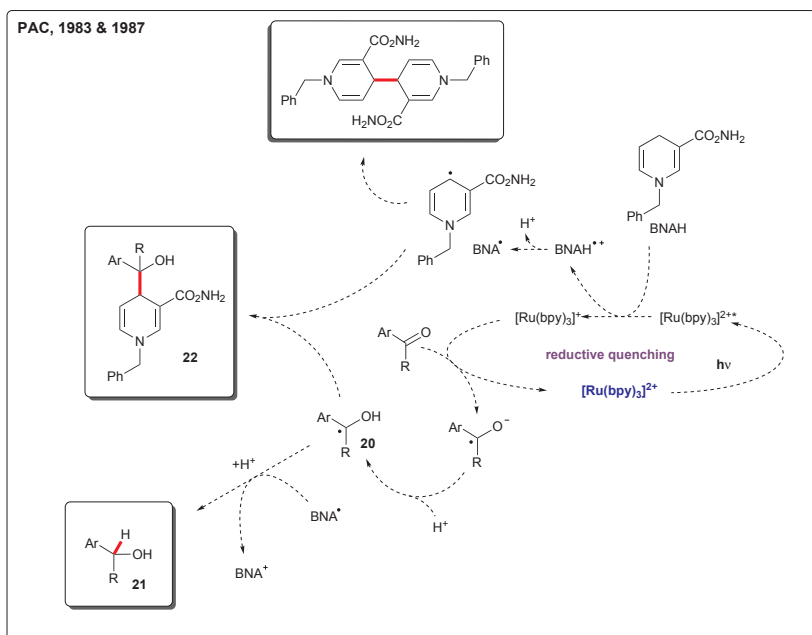
of the used carbonyl compound. Thus, di-2-pyridylketone (17) led to the alcohol 18 together with a dimeric dihydronicotinamide structure 10, whereas benzaldehyde was converted to a secondary alcohol 19 in high



SCHEME 6

$[Ru(bpy)_3]^{2+}$ -photosensitized reactions of carbonyl compounds with an NADH model (refs.<sup>21,22</sup>)

yield. It was reasoned that the exclusive formation of alcohol **18** from di-2-pyridylketone (**17**) is governed by the two pyridyl groups that have a dual role. Because of electron-withdrawing nature of these groups, the one electron reduction of the radical  $\text{HO-C}^\bullet(2\text{-py})_2$  is favored (see single-electron transfer to **20** leading to **21** in Scheme 7). In addition to that, radical coupling of the species **20** (leading to possible product **22**) is inhibited because of steric hindrance around the radical center in  $\text{HO-C}^\bullet(2\text{-py})_2$ .



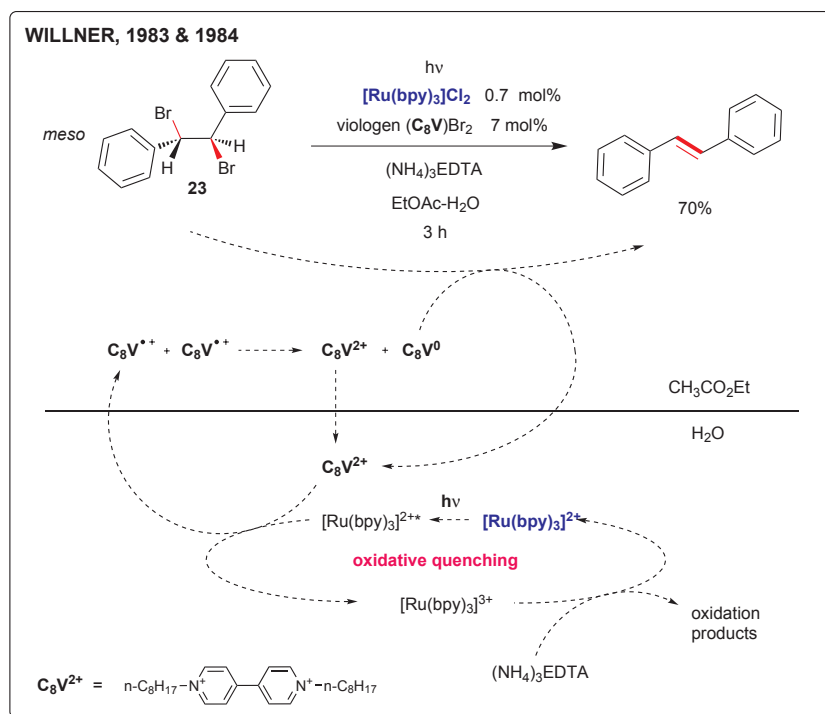
SCHEME 7

Mechanistic picture proposed for transformations of carbonyl compounds in Scheme 6 (refs<sup>21,22</sup>)

Photoinduced electron transfer has been extensively studied because of solar energy conversion and storage<sup>12–14</sup>. In this context, the photoinduced production of 4,4'-bipyridinium radical cations from the corresponding dications (viologens) with visible light is very well-known. Usually,  $[\text{Ru}(\text{bpy})_3]^{2+}$  or zinc porphyrins are used as sensitizers and triethanolamine, ethylenediaminetetraacetic acid (EDTA), or cysteine are introduced as electron donors. Inspired by this, Willner group studied several photochemical transformations involving photogenerated reductant  $[\text{Ru}(\text{bpy})_3]^{2+\bullet}$ <sup>23–25</sup>. Based on their research of viologen/ $\text{Na}_2\text{S}_2\text{O}_4$  reduction system in ethyl acetate–water, they described a photocatalytic version of their debromina-



tion of *meso*-1,2-dibromostilbene (**23**) triggered by light/[Ru(bpy)<sub>3</sub>]<sup>2+</sup> and di(*n*-octyl) viologen (C<sub>8</sub>V<sup>2+</sup>, Scheme 8)<sup>23,24</sup>. Disproportionation of viologen radical cation C<sub>8</sub>V<sup>•+</sup> in ethyl acetate/water biphasic system generates neutral species C<sub>8</sub>V<sup>0</sup> that is believed to be the key reducing agent in the reported debrominations. Interesting enzyme-catalyzed variant of this biphasic photodebromination reaction involves ethanol/alcohol dehydrogenase/NADH reduction system<sup>26</sup>. In this process, enzymatically generated NADH

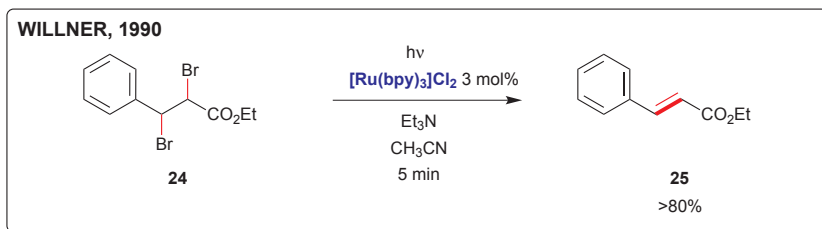


SCHEME 8

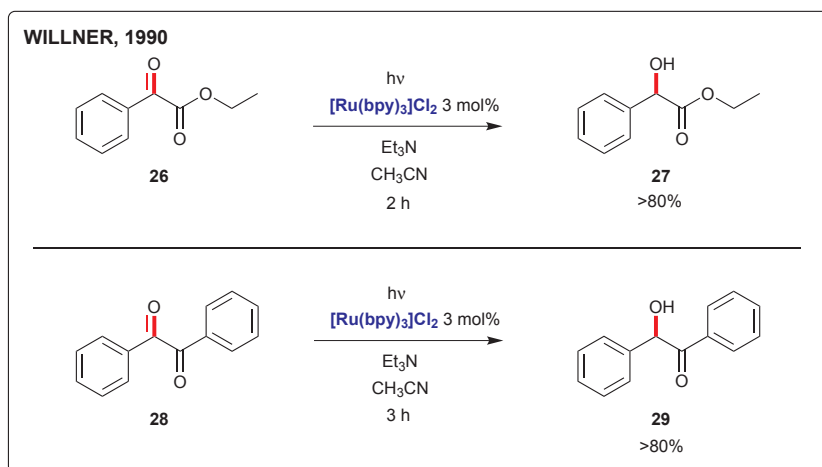
Photosensitized debromination of *meso*-1,2-dibromostilbene in a two-phase system (refs<sup>23,24</sup>)

serves instead of EDTA or other amines to reduce [Ru(bpy)<sub>3</sub>]<sup>3+</sup> to [Ru(bpy)<sub>3</sub>]<sup>2+</sup><sup>27</sup>. Importantly, these reports from Willner group provided early examples showing that oxidative quenching cycle of [Ru(bpy)<sub>3</sub>]<sup>2+\*</sup> by using strong oxidants (e.g. viologens) can be taken advantage of in transformations interesting to organic synthesis. Later on, photocatalysis in the debromination reactions has been also described to proceed with [Ru(bpy)<sub>3</sub>]Cl<sub>2</sub>/Et<sub>3</sub>N in acetonitrile solvent in absence of viologen catalyst (e.g. **24** → **25**, Scheme 9)<sup>28</sup>. Under similar conditions, successful reduction

of activated ketones has been demonstrated (Scheme 10). In this way, ethyl benzoylformate (**26**) is reduced to ethyl mandelate (**27**) and benzil (**28**) to benzoin (**29**).



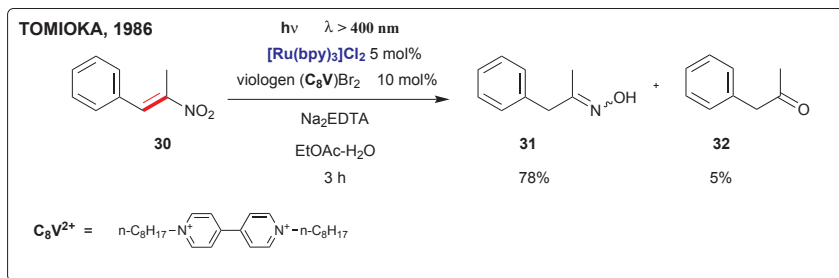
SCHEME 9  
Photocatalyzed debromination of ethyl dibromocinnamate (ref.<sup>28</sup>)



SCHEME 10  
Photocatalyzed reduction of activated ketones triggered by  $[\text{Ru}(\text{bpy})_3]^{2+}/\text{Et}_3\text{N}$  system (ref.<sup>28</sup>)

In 1986, Tomioka group reported examples of reduction of nitroalkenes to oximes using photoredox catalysis with  $[\text{Ru}(\text{bpy})_3]^{2+}$ /viologen/ $\text{Na}_2\text{EDTA}$  system in biphasic medium (Scheme 11)<sup>29</sup>. The corresponding ketones were also isolated in small quantities. Viologen species serves as an electron-phase transfer catalyst shuttling electrons between the aqueous and organic phase and, in this respect, the roles of the ruthenium photocatalyst,  $\text{Na}_2\text{EDTA}$  and viologen are similar to those in the debromination reaction mechanism depicted in Scheme 8. In this case, the authors stated that the reducing species that directly transfers its electrons to the nitroalkene sub-

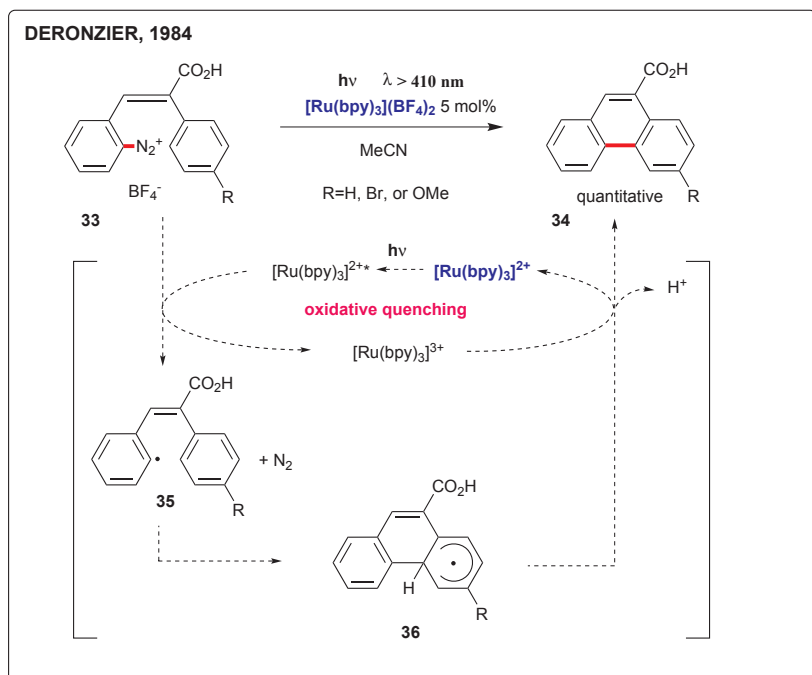
strate is either the viologen radical cation  $C_8V^{•+}$ , or the neutral species  $C_8V^0$  generated by the disproportionation mechanism.



SCHEME 11

Photochemical reduction of nitroalkenes using viologen as an electron-phase transfer catalyst (ref.<sup>29</sup>)

In 1984, Cano-Yelo and Deronzier described photocatalytic Pschorr reaction converting aryldiazonium salts **33** to phenanthrene derivatives **34** in presence of  $[Ru(bpy)_3]^{2+}$  photoredox catalyst (Scheme 12)<sup>30</sup>. The authors

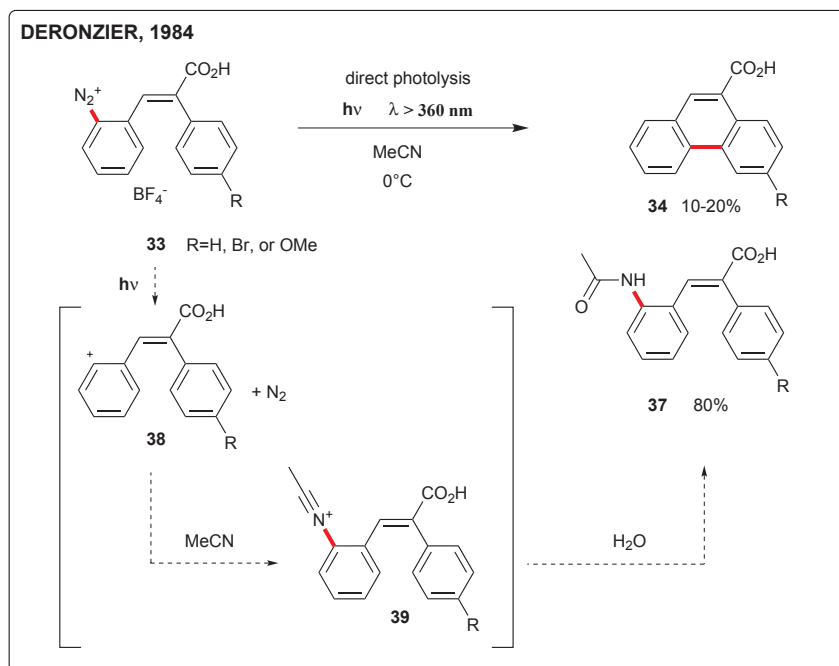


SCHEME 12

Pschorr reaction via visible-light photoredox catalysis with  $[Ru(bpy)_3]^{2+}$  (ref.<sup>30</sup>)

proposed mechanism involving oxidative quenching of photoexcited  $[\text{Ru}(\text{bpy})_3]^{2+*}$  with aryldiazonium salt leading to aryl radical species **35** and  $[\text{Ru}(\text{bpy})_3]^{3+}$  which is a strong oxidant<sup>31</sup>. Radical cyclization of **35** gives intermediate **36**. In the next step, the radical intermediate **36** is oxidized by  $[\text{Ru}(\text{bpy})_3]^{3+}$  and subsequently restores aromaticity upon loss of proton affording phenanthrene skeletons **34**.

Importantly, when the aryldiazonium salts **33** are subjected to direct photolysis in absence of a photoredox catalyst, the phenanthrene products **34** become minor component of the reaction mixture (10–20%, Scheme 13). The major products are acetanilides **37** isolated in 80% yields. They result from interaction of a photogenerated aryl cation **38** with acetonitrile and subsequent hydrolysis of the intermediate **39** (Scheme 13).

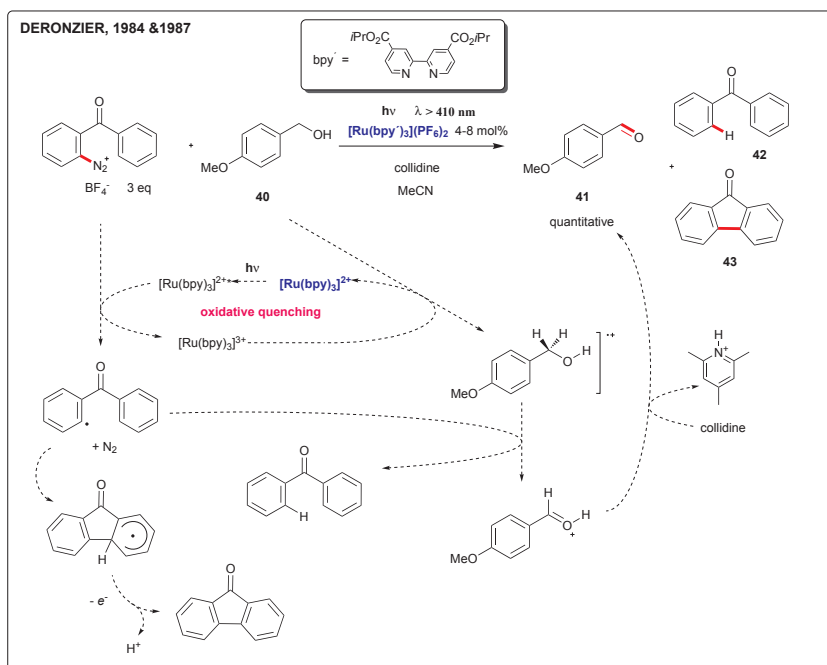


SCHEME 13

Direct photolysis of aryldiazonium salts **33** in absence of a photoredox catalyst and the pathway leading to major acetanilide products **37** via aryl cations **38** (ref.<sup>30</sup>)

The oxidative quenching cycle of Ru-photocatalyst was also used for transformation of carbinols (e.g. **40**, Scheme 14) to aldehydes with aryldiazonium salts as oxidants<sup>32,33</sup>. Besides the aldehyde **41**, this process results in benzophenone **42** and fluorenone **43**, which is a product of the

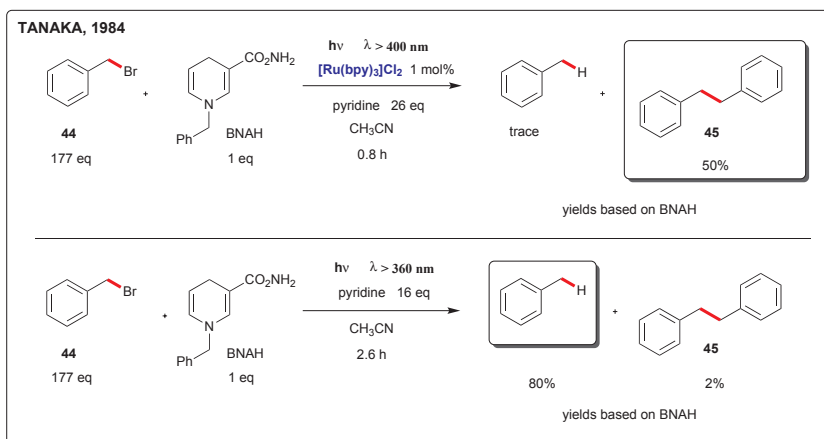
Pschorr cyclization pathway similar to that outlined in Scheme 12. Oxidation of other primary<sup>32</sup> and secondary<sup>33</sup> alcohol substrates was investigated in the presence of various bases and the results were compared with electrochemical variant of this reaction (electrochemical redox catalysis)<sup>33</sup>.



SCHEME 14

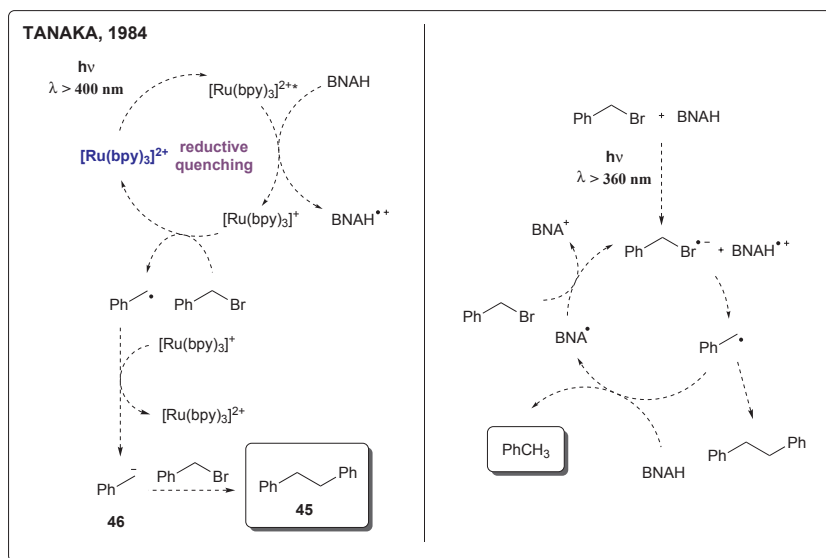
Photooxidation of carbinols to aldehydes via visible-light photoredox catalysis with aryl diazonium salt as a sacrificial oxidant (refs<sup>32,33</sup>)

In 1984, Tanaka group reported a reaction of benzyl bromide (**44**) with 1-benzyl-1,4-dihydronicotinamide (BNAH) photosensitized by  $[\text{Ru}(\text{bpy})_3]^{2+}$  resulting in 1,2-diphenylethane (**45**) as the main product (Scheme 15). However, in absence of  $[\text{Ru}(\text{bpy})_3]^{2+}$  sensitizer, irradiation of the absorption band of BNAH triggers a different photoinduced electron-transfer process leading to reduction of benzyl bromide (**44**) to yield toluene as the major product (Scheme 15 bottom and Scheme 16 right)<sup>34</sup>. Reaction in absence of  $[\text{Ru}(\text{bpy})_3]^{2+}$  proceeds by a radical chain mechanism involving benzyl radical, as the chain carrier, formed by a single-electron transfer from the excited state of BNAH to benzyl bromide (Scheme 16 right). By contrast, in the presence of  $[\text{Ru}(\text{bpy})_3]^{2+}$ , benzyl bromide is subject to two-electron reduction by  $[\text{Ru}(\text{bpy})_3]^+$  generated by reductive quenching of  $[\text{Ru}(\text{bpy})_3]^{2+*}$



SCHEME 15

$[Ru(bpy)_3]^{2+}$ -photosensitized reaction of 1-benzyl-1,4-dihydronicotinamide with benzyl bromide and non-photosensitized process (ref.<sup>34</sup>)



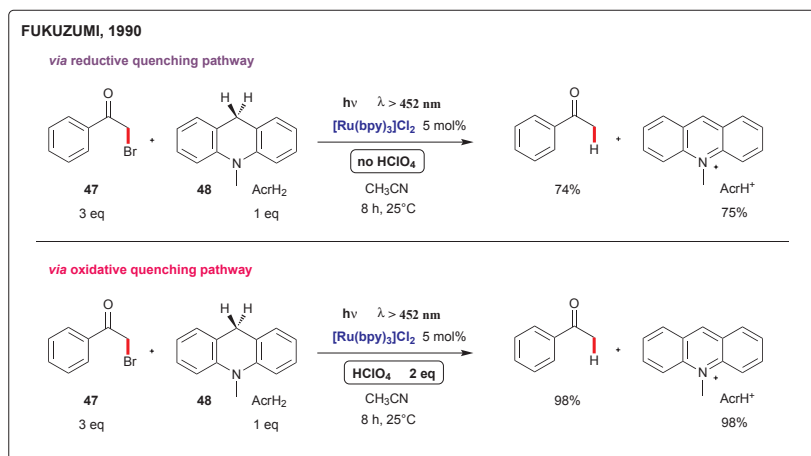
SCHEME 16

Comparison of photoinduced electron-transfer pathways in reaction of benzyl bromide and BNAH in presence (left) and absence (right) of  $[Ru(bpy)_3]^{2+}$  photocatalyst (ref.<sup>34</sup>)

with BNAH (Scheme 16 left). The authors noted there is some similarity between  $[Ru(bpy)_3]^+$  reductant and sodium naphthalenide that can also, as a strong reductant, trigger reduction of benzyl halides to generate anionic

species  $\text{PhCH}_2^-$  (**46**) via two-electron transfer<sup>35a,35b</sup>. In 1987, related photo-assisted C–C coupling of benzyl halide substrates with  $\text{Cu}(\text{dap})_2^+$  photocatalyst ( $\text{dap} = 2,9\text{-bis}(p\text{-anisyl})\text{-}1,10\text{-phenanthroline}$ ) has been described by Kern and Sauvage<sup>35c</sup>. The authors suggested that oxidative quenching pathway of photoexcited  $\text{Cu}(\text{dap})_2^{+*}$  with benzyl halide is operative. Radical coupling of the resulting benzyl radical, or alternatively, two-electron transfer pathway have been proposed as possible mechanistic scenarios.

In 1990, Fukuzumi et al.<sup>36</sup> reported reduction of phenacyl halides by dihydroacridine derivative **48** photocatalyzed by  $[\text{Ru}(\text{bpy})_3]^{2+}$  (Scheme 17).

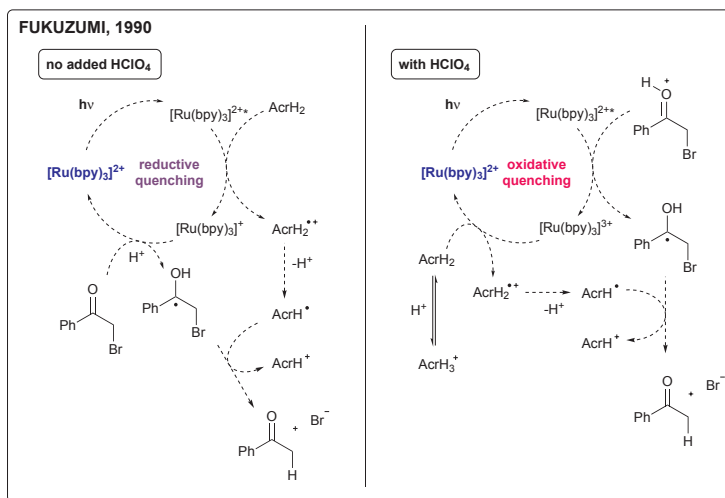


SCHEME 17

$[\text{Ru}(\text{bpy})_3]^{2+}$ -photosensitized reduction of phenacyl bromide by a NADH analogue in absence and presence of acid additive (ref.<sup>36</sup>)

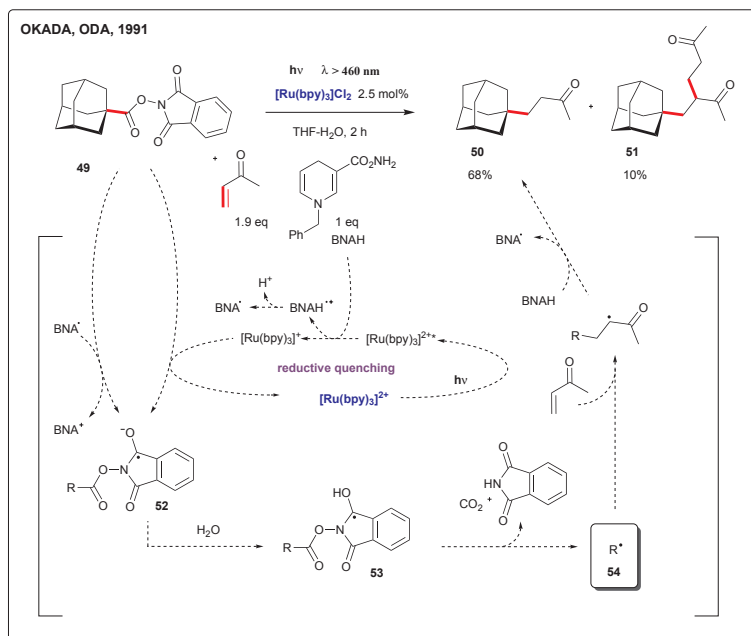
Remarkable influence of perchloric acid on the mechanistic pathway was investigated<sup>37</sup>. In absence of acid, the reaction was found to proceed via reductive quenching of  $[\text{Ru}(\text{bpy})_3]^{2+*}$  by **48** generating  $[\text{Ru}(\text{bpy})_3]^+$  reductant. Conversely, in the presence of perchloric acid, oxidative quenching of  $[\text{Ru}(\text{bpy})_3]^{2+*}$  by phenacyl halides is operative producing  $[\text{Ru}(\text{bpy})_3]^{3+}$  oxidant in situ. The two proposed mechanistic pathways are depicted in Scheme 18.

In 1991, Okada and Oda published a photocatalytic decarboxylative Michael addition of *N*-(acyloxy)phthalimides (Scheme 19)<sup>38</sup>. Reductive quenching of the photoexcited  $[\text{Ru}(\text{bpy})_3]^{2+*}$  with electron rich BNAH leads to strongly reducing  $[\text{Ru}(\text{bpy})_3]^+$  that transfers its electron to phthalimide moiety to generate species **52**. This leads to decarboxylation and generation of the key alkyl radical intermediate **54** and subsequent incorporation of



SCHEME 18

Electron-transfer pathways in reduction of phenacyl halides by dihydroacridine derivative **48** photocatalyzed by  $[\text{Ru}(\text{bpy})_3]^{2+}$  with and without perchloric acid (ref.<sup>36</sup>)



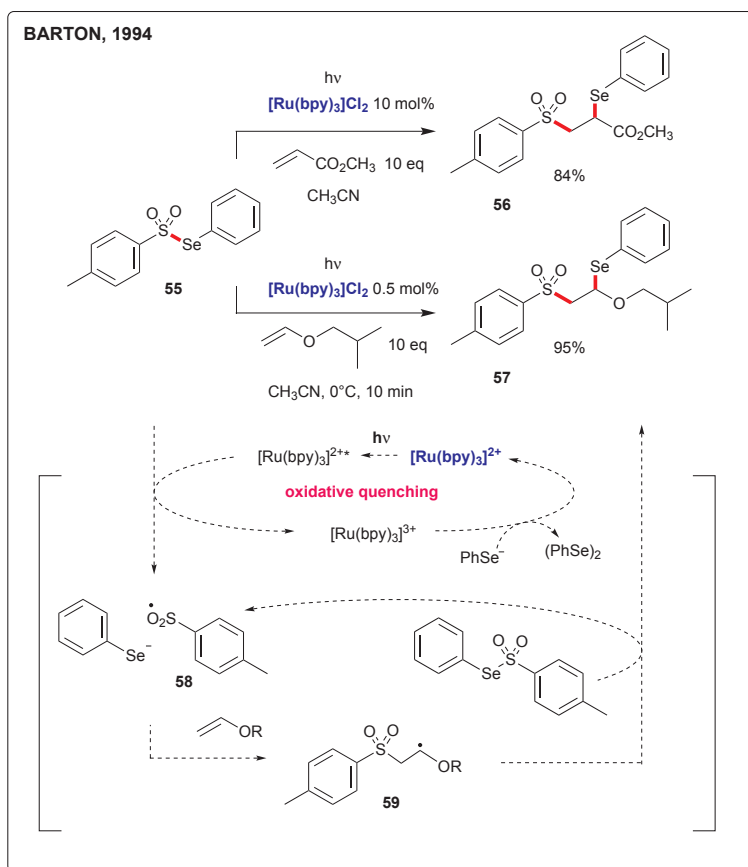
SCHEME 19

Decarboxylative Michael addition of *N*-(acyloxy)phthalimide **49** to electron-deficient olefin (ref.<sup>38</sup>)



Michael acceptors such as methyl vinyl ketone to give products **50** and **51**. In a related work, the key alkyl radical intermediates **54** generated as depicted in Scheme 19 can give rise to reduced species R-H when *t*-BuSH reagent is used as a source of the hydrogen atom<sup>39</sup>. Alternatively the alkyl radicals **54** can be trapped with PhSeSePh to give phenyl selenides R-SePh<sup>40</sup>.

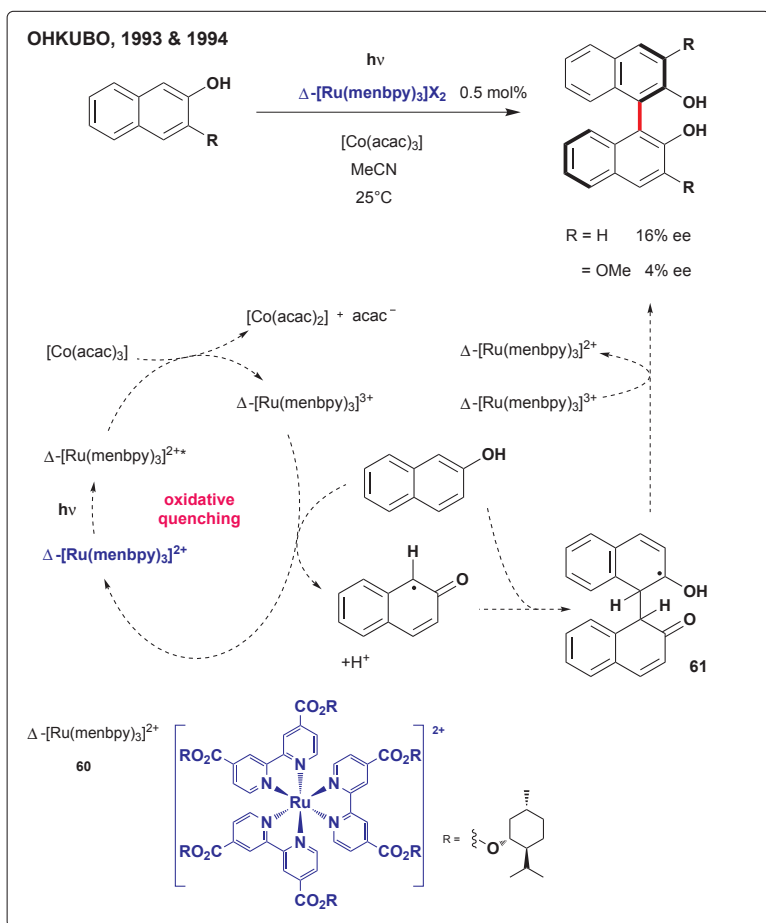
In 1994 Barton et al. reported additions of Se-phenyl *p*-tolueneselenosulfonate **55** to olefins promoted by  $[\text{Ru}(\text{bpy})_3]^{2+}$  and light (Scheme 20)<sup>41</sup>. Oxidative quenching pathway of excited  $[\text{Ru}(\text{bpy})_3]^{2+*}$  with *p*-TolSO<sub>2</sub>SePh (**55**) as the oxidant was proposed to initiate the radical chain reaction (Scheme 20). Electron rich olefins give products such as sulfone **57** in high



SCHEME 20  
 $[\text{Ru}(\text{bpy})_3]^{2+}$ -photocatalyzed addition of Se-phenyl *p*-tolueneselenosulfonate to electron rich olefins (ref.<sup>41</sup>)

yield. Interestingly, transformation  $55 \rightarrow 57$  also worked with  $\text{Ru}(\text{CO})_3\text{Cl}_2$  (86% yield of **57**) and  $[\text{Ru}(\text{bpy})_3]\text{Cl}_2$  catalysts. In this report, the authors predicted that  $[\text{Ru}(\text{bpy})_3]^{2+}$  in combination with light could be used as an initiator for various other radical reactions.

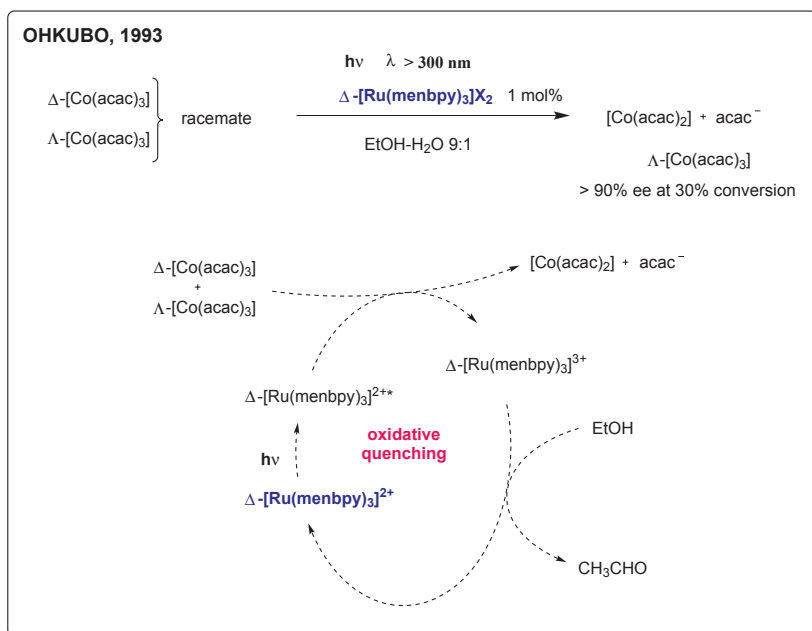
In 1993, Ohkubo et al. devised photoredox catalytic process for oxidative homocoupling of 2-naphthol leading to non-racemic (*R*)-(+)-1,1'-bi-2-naphthol (BINOL)<sup>42,43</sup>. Visible-light irradiation of the substrate in presence of enantiopure  $\Delta$ -[Ru(menbpy)<sub>3</sub>]<sup>2+</sup> **60** afforded non-racemic BINOL with 16% ee (Scheme 21). In this transformation, that features oxidative



SCHEME 21

Enantioselective oxidative homocoupling of 2-naphthol by photoredox catalysis with  $\Delta$ -[Ru(menbpy)<sub>3</sub>]<sup>2+</sup> (refs<sup>42,43</sup>)

quenching pathway of the excited ruthenium photocatalyst,  $[\text{Co}(\text{acac})_3]$  was used as a sacrificial oxidant. As the authors proposed, the enantioselectivity is presumably governed by the counterclockwise molecular helicity along the  $C_3$  axis of the ruthenium complex during the oxidation of the radical intermediate **61**. Remarkably, the ruthenium photocatalytic system based on  $[\text{Ru}(\text{menbpy})_3]^{2+}$  is able to trigger a very efficient enantioselective photocatalytic reduction of  $[\text{Co}(\text{acac})_3]$  (Scheme 22)<sup>44</sup>.  $\Delta$  enantiomer of the octahedral complex  $[\text{Co}(\text{acac})_3]$  reacts considerably faster as compared to the  $\Lambda$  enantiomer.



SCHEME 22

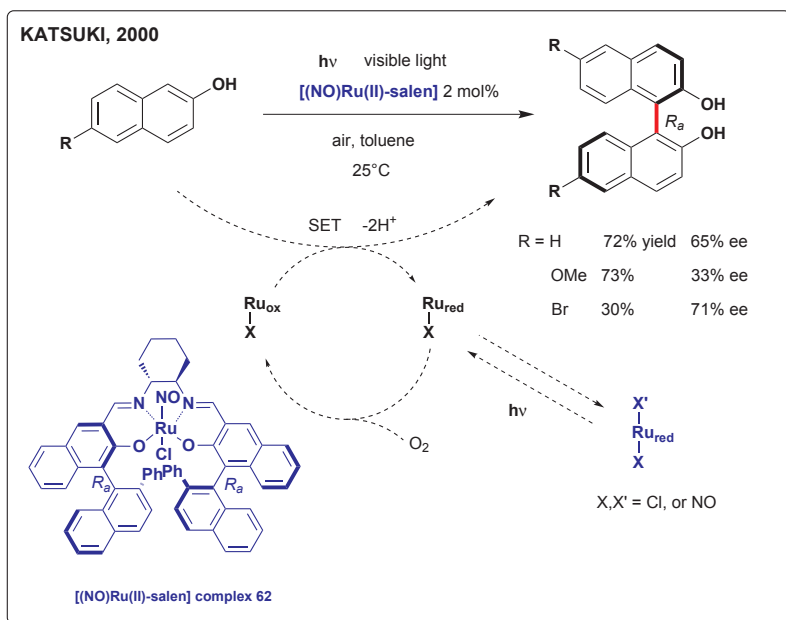
Enantioselective decomposition of  $[\text{Co}(\text{acac})_3]$  by photocatalysis with  $\Delta\text{-}[\text{Ru}(\text{menbpy})_3]^{2+}$  (ref.<sup>44</sup>)

This transformation proceeds via oxidative quenching of the enantiopure ruthenium photocatalyst with racemic  $[\text{Co}(\text{acac})_3]$ , that occurs with a significantly different rate for the  $\Delta$  and  $\Lambda$  enantiomer in the mixture of ethanol–water 9:1 ( $k_\Delta/k_\Lambda = 14.7$ ). With the rate being larger for consumption of  $\Delta\text{-}[\text{Co}(\text{acac})_3]$ , the reaction mixture can be enriched in  $\Lambda\text{-}[\text{Co}(\text{acac})_3]$  enantiomer (up to 94% ee at 30% conversion). Notably strong dependence on the composition of the solvent system has been observed. When the content of ethanol in the solvent system has been decreased to 8:1 relative

to water, the ratio of the individual enantiomer consumption rates decreased considerably to  $k_{\Delta}/k_{\Lambda} = 8.7$ .

In a related work Ohkubo group described enantioselective photoredox synthesis of  $[\text{Co}(\text{acac})_3]$  from racemic  $[\text{Co}(\text{acac})_2(\text{H}_2\text{O})_2]$  and acetylacetone using various non-racemic ruthenium photocatalysts in ethanol/water solvent system in the presence of molecular oxygen<sup>45</sup>. The best catalyst was  $\Delta$ - $[\text{Ru}(\text{menbpy})_3]^{2+}$  with which they achieved 37% ee in favor of  $\Lambda$ - $[\text{Co}(\text{acac})_3]$  enantiomer. The authors proposed a reaction pathway, where the excited state of the ruthenium catalyst is oxidatively quenched by the molecular oxygen to generate strongly oxidizing  $\Delta$ - $[\text{Ru}(\text{menbpy})_3]^{3+}$ . This in turn triggers the enantioselective key step that involves non-equal rates of formation of the individual enantiomers of  $[\text{Co}(\text{acac})_3]$  favoring  $\Lambda$ - $[\text{Co}(\text{acac})_3]$  enantiomer. Although the previous examples by Ohkubo are more from the realm of inorganic chemistry, they might be inspiring to organic chemists interested in enantioselective electron transfer reactions<sup>46</sup>.

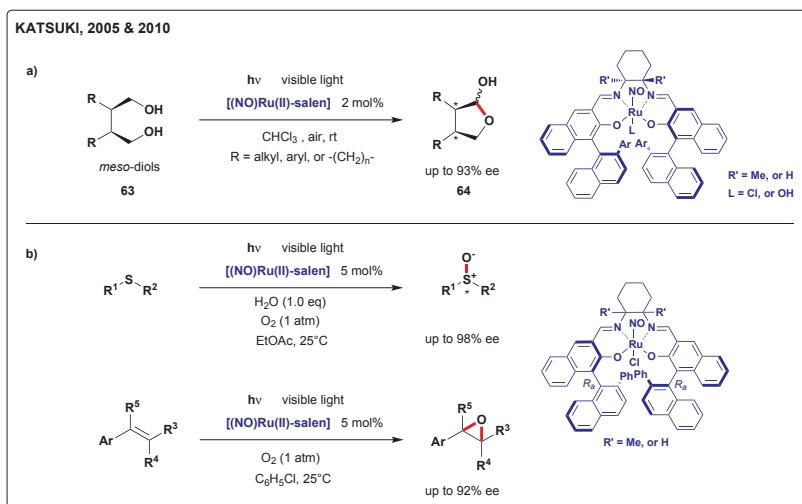
In 2000, group of Katsuki published work on enantioselective oxidative homocoupling of phenolic substrates using a different ruthenium catalytic system based on  $[(\text{NO})\text{Ru}(\text{II})\text{-salen}]$  motif (Scheme 23)<sup>47,48</sup>. The reaction



SCHEME 23

Enantioselective oxidative dimerization of 2-naphthol by catalysis with  $[(\text{NO})\text{Ru}(\text{II})\text{salen}]$  complex **62** in the presence of molecular oxygen (ref.<sup>47</sup>)

mixture was irradiated with 150 W halogen lamp in presence of molecular oxygen and the enantioselectivities achieved for various BINOLs ranged from 30 to 71%. The authors provided a mechanistic outline depicted in Scheme 23. Light was proposed to induce release of the nitrosyl ligand from the ruthenium center of the precatalyst. However, it was not disclosed at this point if the light can play an active role also during the key single-electron transfer steps in the catalytic cycle. Importantly, investigation of another oxidation reaction catalyzed by Ru(II)-salen system by Katsuki<sup>49a</sup> showed that light can participate in certain single-electron transfer steps involving this catalyst. In this report, enantioselective desymmetrization of meso-diols leading to non-racemic lactols under visible-light photo-irradiation<sup>49a</sup> was disclosed (e.g. **63** → **64**, Scheme 24). The mechanism of this transformation has been studied in great detail and spectroscopic analysis revealed that irradiation with visible light was indispensable not only to trigger dissociation of the nitrosyl ligand but also to promote single-electron transfer from the alcohol-bound ruthenium ion to molecular oxygen. Fine ligand tuning of the ruthenium(salen) complexes was required to achieve high enantioselectivities (up to 93% ee).



SCHEME 24

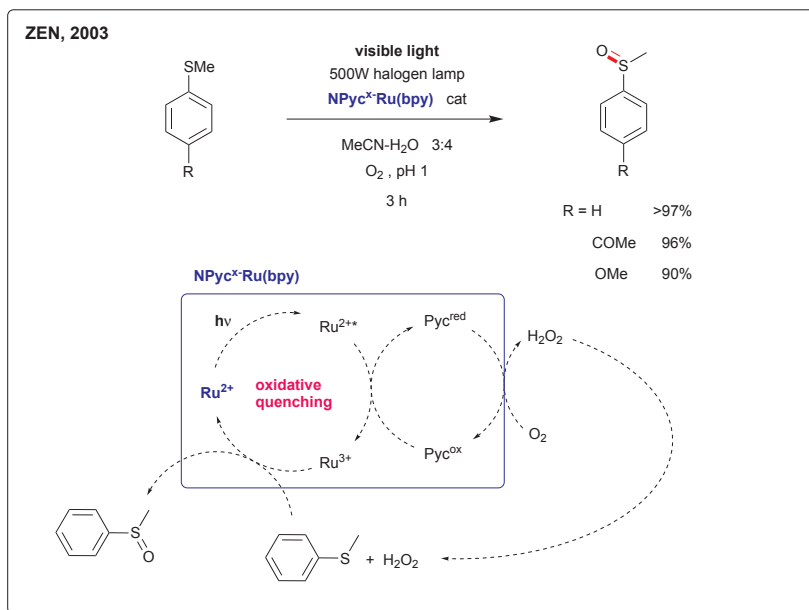
a) Aerobic oxidative desymmetrization of meso-diols promoted by [(NO)Ru(II)-salen] photocatalysts (ref. <sup>49a</sup>). b) Asymmetric aerobic sulfide oxidation and epoxidation (ref. <sup>49b</sup>)

Very recently, Katsuki group reported a detailed study<sup>49b</sup> on photo-promoted Ru-catalyzed asymmetric aerobic sulfide oxidation and epoxidation. Oxidation of various sulfides using again ruthenium(salen) complexes

as the catalysts proceeded with enantioselectivities of up to 98% ee. The epoxidation of conjugated olefins showed also moderate to high enantioselectivities (76–92% ee, Scheme 24). The role of water as a proton-transfer mediator has been investigated.

#### 4. PHOTOREDOX CATALYSIS IN THE FIRST DECADE OF THE 21st CENTURY

In 2003, Zen group reported a clean and selective photocatalytic oxidation of sulfides to sulfoxides. A heterogeneous nafion membrane doped with a lead ruthenate pyrochlore catalyst (Pyc) and  $[\text{Ru}(\text{bpy})_3]^{2+}$  photosensitizer (designated as  $\text{NPyc}^x\text{-Ru}(\text{bpy})$ ) was used to achieve selective sulfoxide formation with no overoxidation to the sulfone (Scheme 25)<sup>50</sup>. The success of this system lies in the combination of catalyst, photosensitizer, solvent



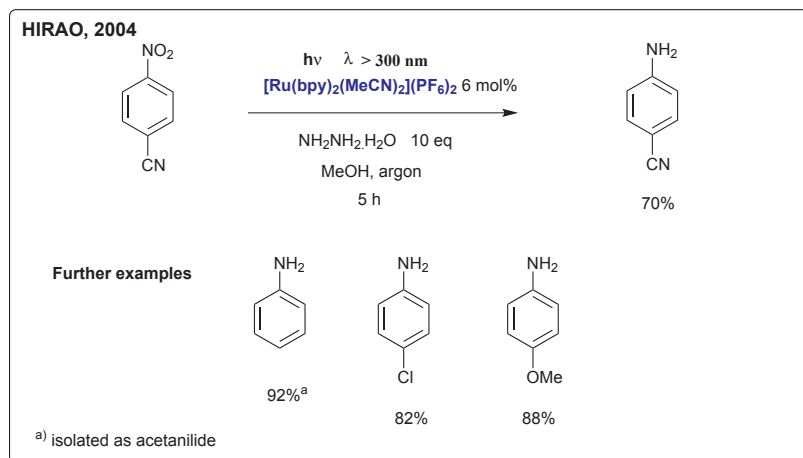
SCHEME 25

Photocatalytic oxidation of sulfides to sulfoxides catalyzed by doped nafion membrane  $\text{NPyc}^x\text{-Ru}(\text{bpy})$  (ref.<sup>50</sup>)

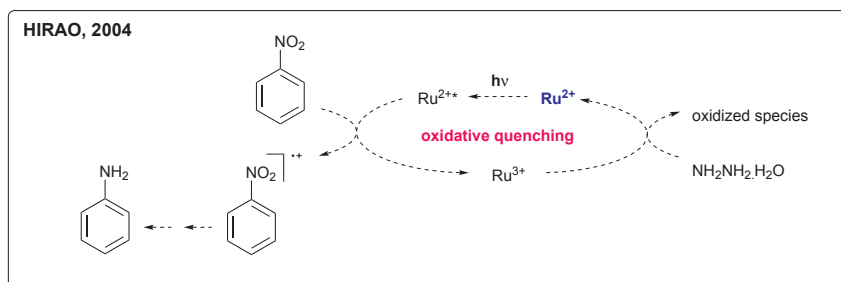
composition, pH value, molecular oxygen, and light illumination. In a proposed mechanistic scheme, Pyc plays a dual catalytic role in the dioxygen reduction to generate  $\text{H}_2\text{O}_2$  and as an oxidant in the oxidative quenching of the photoexcited ruthenium species ( $\text{Ru}^{2+*}$ ). Hydrogen peroxide then serves as an oxidant for sulfide to sulfoxide oxidation. Purging of the sys-

tem with  $O_2$  proved to be essential for the formation of  $H_2O_2$  during the reaction. The control experiment with 30%  $H_2O_2$  solution gave only about 47% conversion with poor selectivity.

In 2004, Hirao group published photoinduced reduction of nitrobenzenes with hydrazine hydrate in presence of  $[Ru(bpy)_3]Cl_2$  or related catalysts<sup>51</sup>. Among them,  $[Ru(bpy)_2(MeCN)_2](PF_6)_2$  was the most efficient and gave the best yields of anilines with both electron-withdrawing and -donating substituents (Scheme 26). The authors proposed oxidative quenching pathway during which photoexcited ruthenium catalyst gets oxidized by the nitro-compound (Scheme 27). Corresponding anilines were isolated in good



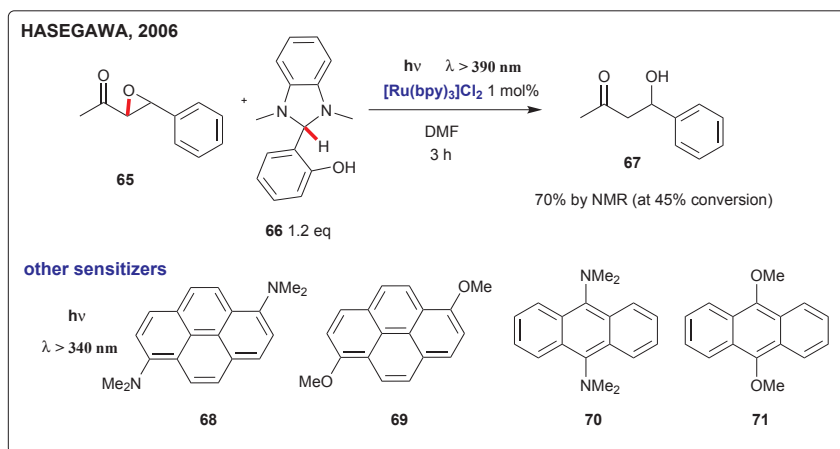
SCHEME 26  
Reduction of nitrobenzenes to anilines using hydrazine hydrate reductant and ruthenium photocatalyst (ref.<sup>51</sup>)



SCHEME 27  
Oxidative quenching pathway proposed for photoexcited ruthenium catalyst in reduction of nitrobenzenes with hydrazine hydrate (ref.<sup>51</sup>)

yields and cyano group was reported to stay intact in this process. The initial study with parent nitrobenzene showed that methanol is a suitable solvent while reduced efficiency was observed with  $\text{CH}_2\text{Cl}_2$  (GC yields 99 and 52%, respectively). Use of THF and acetonitrile led to drastically diminished yields (GC: 18 and 12%).

In 2006, Hasegawa group reported a study on photoinduced electron-transfer (PET) reactions of several ketones in presence of organic photosensitizers such as substituted pyrenes and anthracenes **68–71** cooperating with 2-aryl-1,3-imidazolines as reductants (e.g. **66**, Scheme 28)<sup>52</sup>. In a reductive epoxide opening **65**  $\rightarrow$  **67** also  $[\text{Ru}(\text{bpy})_3]\text{Cl}_2$  has been investigated besides purely organic photosensitizers **68–71**.

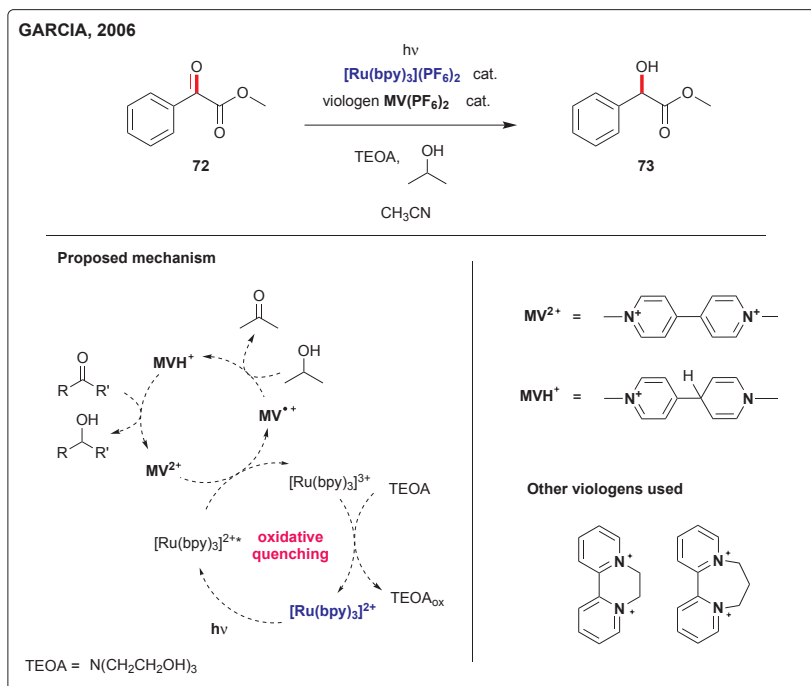


SCHEME 28

Photoinduced electron-transfer reduction of epoxide triggered by  $[\text{Ru}(\text{bpy})_3]^{2+}$ /2-aryl-1,3-imidazolines (ref.<sup>52</sup>)

In 2006, intriguing photocatalytic Meerwein–Ponndorf–Verley-type (MPV) reduction using a  $[\text{Ru}(\text{bpy})_3]^{2+}$ /viologen couple has been disclosed by Garcia group (Scheme 29)<sup>53</sup>. Oxidative quenching catalytic cycle has been proposed involving oxidation of photoexcited  $[\text{Ru}(\text{bpy})_3]^{2+*}$  by viologen species. The reduced viologen  $\text{MVH}^+$  (Scheme 29) was suggested to transfer hydride to carbonyl substrate resulting in alcohol product. The proposed mechanism invites to investigate enantioselective variants of this photocatalytic MPV process with chiral non-racemic viologen catalysts. Interestingly, there is some relation of this work to studies by Willner<sup>23,24,28</sup> (Schemes 8–10), where alternative conditions and mechanistic pathways are discussed.

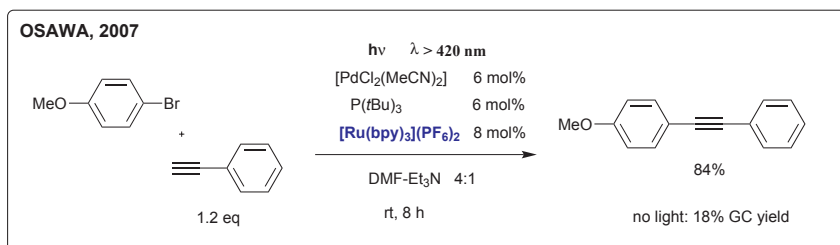




SCHEME 29

Photocatalytic Meerwein–Ponndorf–Verley-type reduction of ketones using a [Ru(bpy)<sub>3</sub>]<sup>2+</sup>/viologen couple (ref.<sup>53</sup>)

In 2007, Osawa group published visible-light promoted copper-free Sonogashira coupling reaction of aryl bromides at room temperature using [Ru(bpy)<sub>3</sub>]<sup>2+</sup> photocatalyst (Scheme 30)<sup>54</sup>. When irradiated, 4-bromoanisole and phenylacetylene gave Sonogashira coupling product in 84% isolated yield, whereas the same reaction run in the dark led to only 18% yield (GC



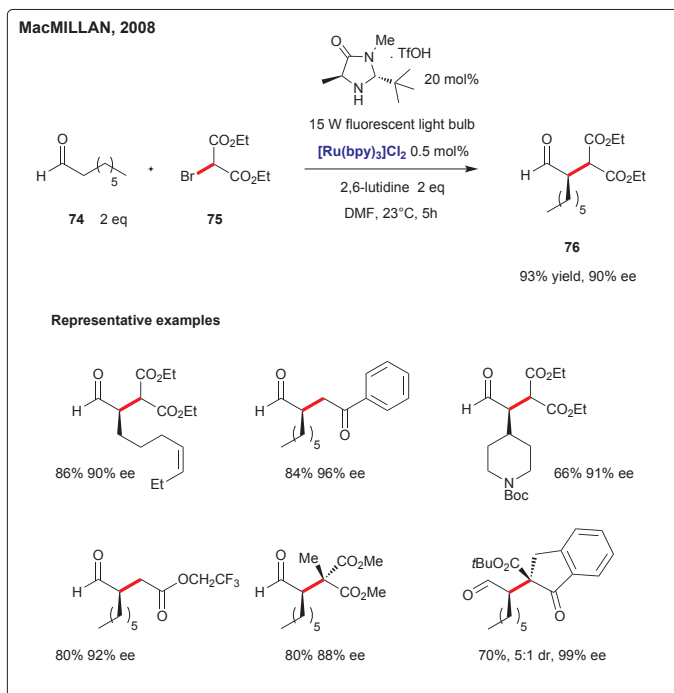
SCHEME 30

Light-promoted copper-free Sonogashira coupling reaction (ref.<sup>54</sup>)

yield, Scheme 30). The  $[\text{Ru}(\text{bpy})_3]^{2+}$  photocatalyst has been suggested to take part in the formation of Pd(0) species from the Pd(II) precursor and also during oxidative addition of arylbromide. Notably, when the light is turned off, the coupling reaction slows down significantly and accelerates again after irradiation is resumed. Osawa work represents a unique example of metal-catalyzed coupling reaction promoted by visible light.

Since 2008, the development of methods exploring visible-light photoredox catalysis for organic synthesis experienced remarkable acceleration. This latest work from groups of MacMillan<sup>5,55,56</sup>, Yoon<sup>6,57–59</sup>, Stephenson<sup>7,60–65</sup>, Koike and Akita<sup>66</sup>, Gagné<sup>67</sup>, Zeitler<sup>8</sup> and Rueping<sup>68</sup> is turning this strategy into a powerful synthetic tool.

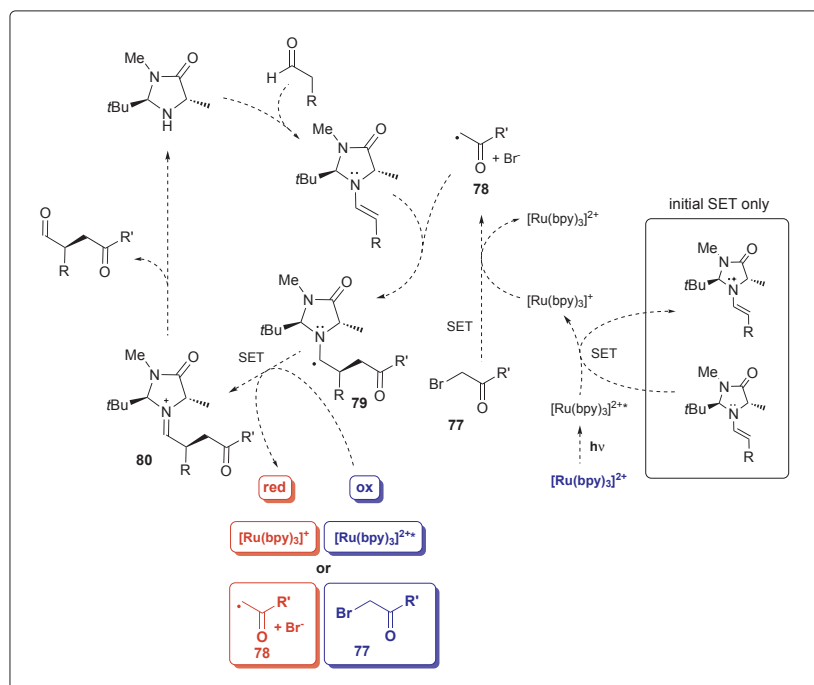
In 2008, MacMillan group demonstrated that photoredox catalysis using  $[\text{Ru}(\text{bpy})_3]\text{Cl}_2$  can be merged with amine organocatalysis<sup>4,5</sup>, specifically singly occupied molecular orbital (SOMO) catalysis<sup>69</sup>. This seminal work introduced a powerful concept that offers many opportunities for asymmetric transformations. Intermolecular  $\alpha$ -alkylation of aldehydes (Scheme 31) was



SCHEME 31

Direct  $\alpha$ -alkylation of aldehydes by merging amine organocatalysis with  $[\text{Ru}(\text{bpy})_3]^{2+}$  photoredox catalysis to achieve asymmetric C–C bond formation (ref.<sup>5</sup>)

proposed to proceed via enamine activation mode for the aldehyde substrate cooperating with photoredox manifold of  $[\text{Ru}(\text{bpy})_3]^{2+}$  (Scheme 32)<sup>5</sup>. In this work, SOMO concept earlier introduced by MacMillan took a new direction. To initiate the reaction, sacrificial quantity of enamine has been proposed to serve as a reductive quencher of the photoexcited  $[\text{Ru}(\text{bpy})_3]^{2+*}$  to generate strongly reducing  $[\text{Ru}(\text{bpy})_3]^+$  ( $-1.33$  V vs SCE in  $\text{CH}_3\text{CN}$ ). This species will be able in turn to transfer electron onto  $\alpha$ -bromocarbonyl substrate **77** to produce electron deficient radical **78** and regenerate  $[\text{Ru}(\text{bpy})_3]^{2+}$  ( $E_{1/2}$  for phenacyl bromide =  $-0.49$  V vs SCE in  $\text{CH}_3\text{CN}$ ). Electron deficient radical **78** has been proposed to attack electron-rich SOMOphilic enamine to give radical intermediate **79** with a substantial tendency to lose electron ( $-0.92$  to  $-1.12$  V vs SCE in  $\text{CH}_3\text{CN}$ ). Subsequent oxidation of this species leading to iminium **80** via single-electron transfer onto  $[\text{Ru}(\text{bpy})_3]^{2+*}$  to generate  $[\text{Ru}(\text{bpy})_3]^+$  (ox  $\rightarrow$  red, Scheme 32) has been proposed. Alternatively, radical intermediate **79** can transfer its electron to another molecule of  $\alpha$ -bromocarbonyl **77**<sup>4b</sup>. Although the plausible mecha-

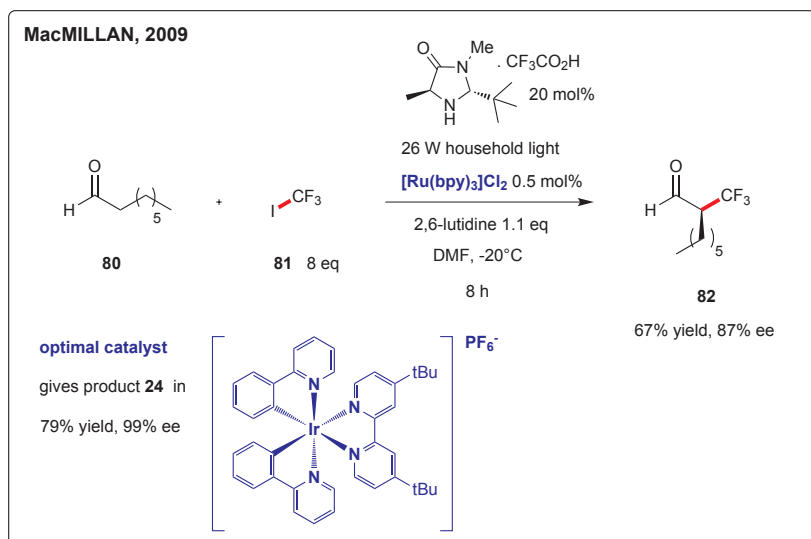


SCHEME 32

Merging amine catalysis and organometallic photoredox catalysis to achieve asymmetric C-C bond formation

nistic picture of the transformation has been outlined, the details of this intricate photoredox process that combines two modes of activation are not fully established at the moment and will therefore require more extensive mechanistic study.

Photoredox organocatalysis is also a powerful way to accomplish challenging enantioselective  $\alpha$ -trifluoromethylation and  $\alpha$ -perfluoroalkylation of aldehydes (e.g. **80**  $\rightarrow$  **82**, Scheme 33)<sup>55</sup> using a readily available iridium photocatalyst and a commercial imidazolidinone catalyst. The presence of 2,6-lutidine is necessary to remove hydroiodic acid that is formed during the reaction. Although  $[\text{Ir}(\text{ppy})_2(\text{dtb-bpy})]\text{PF}_6$  was found to be the optimal photocatalyst, commercially available  $[\text{Ru}(\text{bpy})_3]\text{Cl}_2$  could also be used to afford the desired products in slightly diminished yields and enantioselectivities (ppy = 2-phenylpyridinato-C2,N, dtb-bpy = 4,4'-di-*tert*-butyl-2,2'-bipyridine). The resulting  $\alpha$ -trifluoromethyl aldehydes were subsequently shown as versatile precursors for the construction of a variety of enantioenriched trifluoromethylated building blocks.

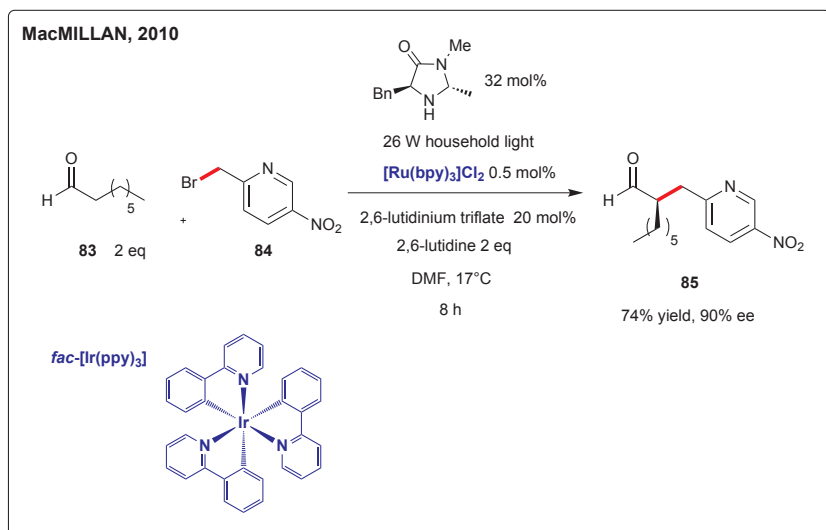


SCHEME 33

Enantioselective  $\alpha$ -trifluoromethylation of aldehydes by merging amine organocatalysis with photoredox catalysis (ref.<sup>55</sup>)

In 2010, enantioselective aldehyde  $\alpha$ -benzylation using electron-deficient aryl and heteroaryl substrates has been accomplished (e.g. **83**  $\rightarrow$  **85**, Scheme 34)<sup>56</sup>. Majority of example transformations proceed best with *fac*- $[\text{Ir}(\text{ppy})_3]$  photocatalyst (ppy = 2-phenylpyridinato-C2,N). Nevertheless,

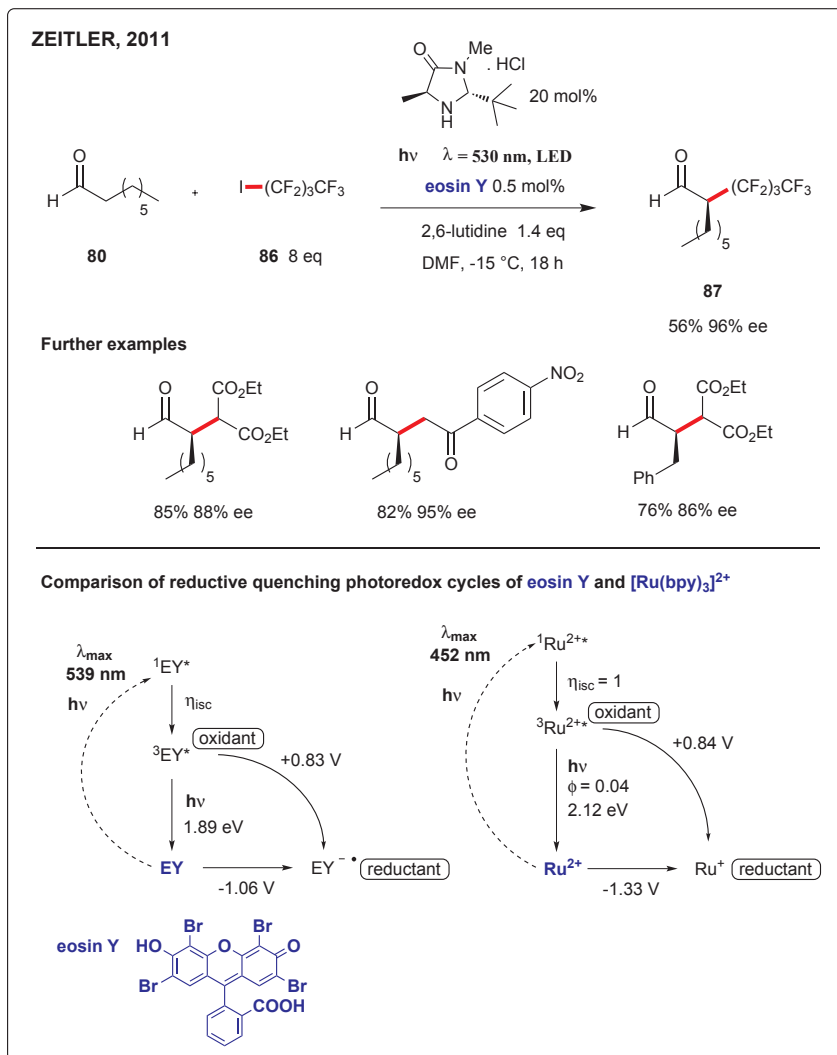
$[\text{Ru}(\text{bpy})_3]\text{Cl}_2$  works also as a competent photoredox catalyst in this process albeit usually with lower conversions. This strategy directly allows the stereocontrolled formation of compounds with homobenzylic stereogenic centers in good to excellent yield under mild conditions.



SCHEME 34  
Enantioselective  $\alpha$ -benzylation of aldehydes via photoredox organocatalysis (ref.<sup>56</sup>)

Important extension of the enantioselective photoredox  $\alpha$ -perfluoroalkylation and  $\alpha$ -alkylation concept has been published in 2011 by Zeitler et al.<sup>8</sup>. The authors demonstrated that the merger of amine organocatalysis with photoredox catalysis can be achieved in presence of purely organic photosensitizers such as eosin Y (Scheme 35). Photoredox catalysis using eosin Y<sup>70</sup> thus represents fully organocatalytic variant of the MacMillan intermolecular  $\alpha$ -alkylation of aldehydes. Notably, eosin Y (EY) undergoes photoredox steps that are comparable to  $[\text{Ru}(\text{bpy})_3]^{2+}$  (Scheme 35 bottom) suggesting similar catalytic pathways in the two cases (cf. Schemes 32 and 35). Interestingly, it has been noticed in this study that  $\alpha$ -alkylation continues to proceed even after the initial irradiation is stopped (“dark reaction”)<sup>8</sup>. Electron transfer from **79** onto  $\alpha$ -bromocarbonyl substrate **77** to regenerate reactive radical **78** might account for this observed “dark” propagation of the reaction (Scheme 32). Such regeneration of the SOMophilic species **78** during the production of iminium **80** will imply that the overall reaction is a radical chain process and light would only be needed to initi-

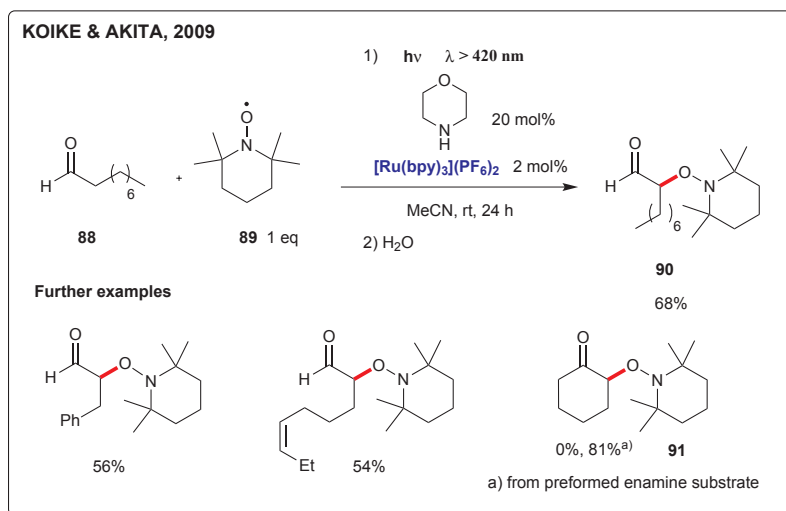
ate the reaction in such a pathway (Scheme 32). The data by Zeidler et al. therefore raised interesting questions about what is the role of light and photocatalyst during the various stages of such mechanistically complex photoredox processes.



SCHEME 35

Purely organocatalytic enantioselective  $\alpha$ -perfluoroalkylation and  $\alpha$ -alkylation of aliphatic aldehydes using eosin Y as photoredox catalyst (ref.<sup>8</sup>)

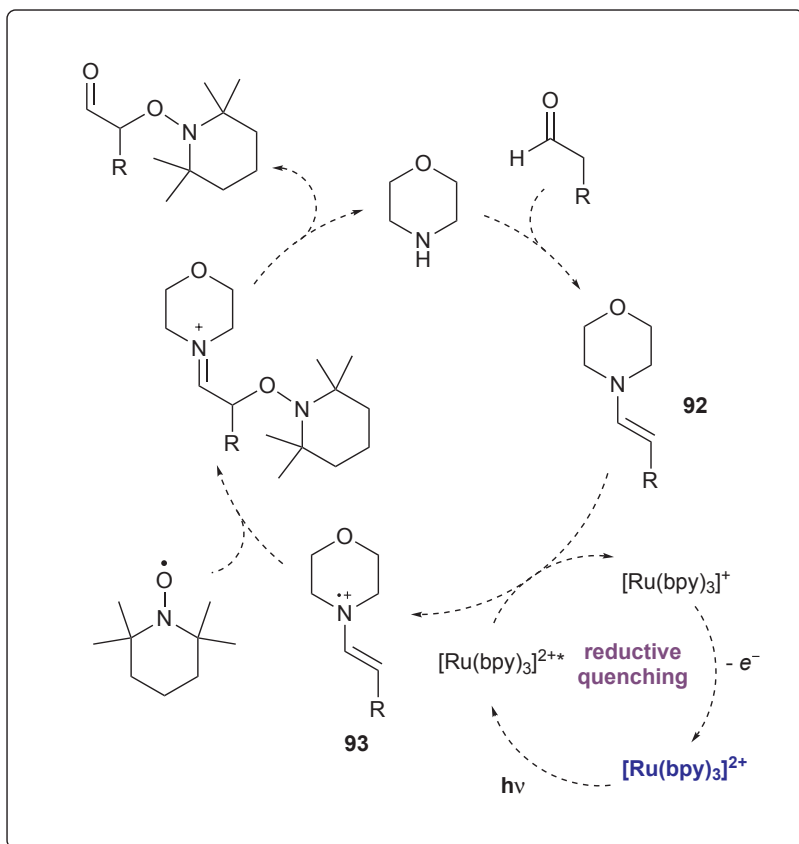
In 2009, Koike and Akita described  $\alpha$ -oxyamination of aldehydes with TEMPO using photoredox catalysis with  $[\text{Ru}(\text{bpy})_3]^{2+}$  (e.g. **88**  $\rightarrow$  **90**, Scheme 36)<sup>66</sup>. In this transformation, activation mode of the aldehyde



SCHEME 36  
 Photocatalytic oxyamination of aldehydes with TEMPO (ref.<sup>66</sup>)

with morpholine is beneficially combined with the photoredox pathway of Ru photocatalyst. The authors suggested a mechanistic scenario depicted in Scheme 37. The enamine **92** formed in situ was proposed to reductively quench the  $[\text{Ru}(\text{bpy})_3]^{2+*}$  species to generate radical cation **93** that further reacts with TEMPO to give oxyaminated aldehyde product. The  $[\text{Ru}(\text{bpy})_3]^+$  generated during the reductive quench should be reoxidized to  $[\text{Ru}(\text{bpy})_3]^{2+}$  with an electron acceptor that has not been specified. Interestingly, cyclohexanone gave no  $\alpha$ -oxyamination product **91** under the conditions described in Scheme 36. However, enamine substrate preformed from cyclohexanone and morpholine underwent the reaction smoothly giving 81% yield of the expected product **91**.

In 2008, Yoon group introduced intramolecular enone [2+2] cycloadditions triggered by visible-light photocatalysis (Scheme 38)<sup>6</sup>. A variety of aryl enones have been shown to undergo readily this transformation, and the diastereoselectivity in the formation of the cyclobutane products was excellent. The authors proposed a mechanism in which a photogenerated  $[\text{Ru}(\text{bpy})_3]^+$  complex promotes one-electron reduction of the enone substrate, which undergoes subsequent radical anion cycloaddition. The reac-

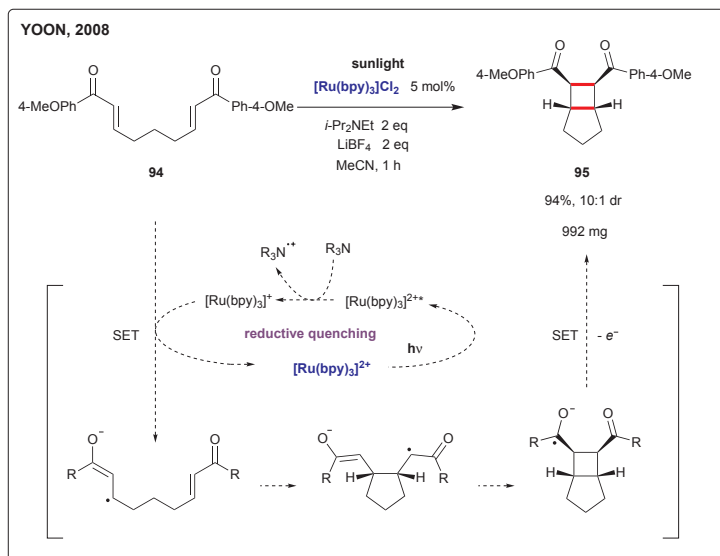


SCHEME 37

Proposed mechanistic pathway of photocatalytic  $\alpha$ -oxyamination of aldehydes with TEMPO

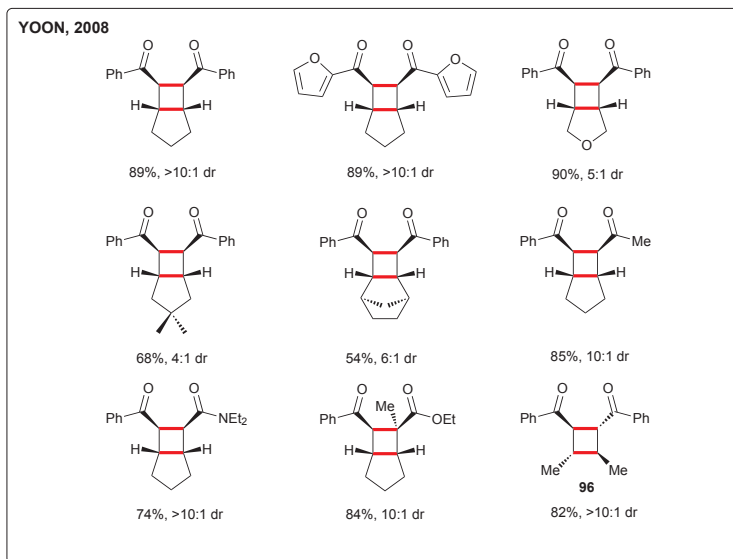
tion can be conducted using incident sunlight as the only source of irradiation. No reaction was observed in the absence of *i*-Pr<sub>2</sub>NEt, even upon extended irradiation with higher catalyst loadings (5 h, 20 mole %  $[\text{Ru}(\text{bpy})_3]\text{Cl}_2$ ). This suggests that cycloaddition is not directly initiated by the photoexcited  $[\text{Ru}(\text{bpy})_3]^{2+*}$  state but rather that the catalytically relevant reductant is a  $[\text{Ru}(\text{bpy})_3]^+$  species formed upon reductive quenching by the amine. The lithium salt was suggested to function as a Lewis acid in this reaction activating the enone toward one-electron reduction. It is of note, that this work was inspired by the radical anion cyclization step with bis(enone) substrates that has been previously pioneered by Krische and Bauld in a different context of one-electron reductions with cobalt<sup>71a,71b</sup>, and copper catalysts<sup>71c</sup>, and also upon cathodic<sup>71d</sup> and homogeneous<sup>71e</sup>





SCHEME 38

Visible-light photocatalysis of bis(enone) [2+2] cycloadditions via reductive quenching of photoexcited  $[\text{Ru}(\text{bpy})_3]^{2+*}$  state (ref.<sup>6</sup>)

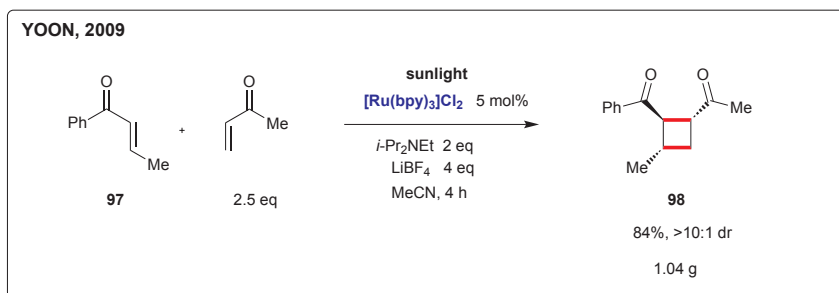


SCHEME 39

Selected products prepared by [2+2] cycloaddition via photoredox catalysis (ref.<sup>6</sup>)

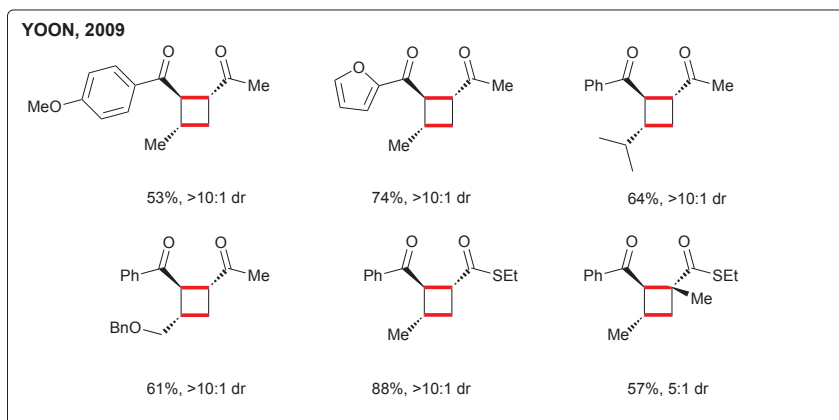
one-electron reductions. Finally, in this work Yoon and coworkers also studied intermolecular [2+2] homodimerizations that were found to proceed smoothly (Scheme 39)<sup>6</sup>. Here, C<sub>2</sub> symmetric products such as **96** were produced, which was in contrast to the tethered intramolecular reactions.

In a related work, challenging crossed intermolecular [2+2] cycloaddition of two different enones was accomplished (Scheme 40)<sup>57</sup>. With this method, a diverse range of non-symmetric tri- and tetrasubstituted cyclobutane structures was produced in good yields and diastereoselectivities (Scheme 41). Importantly, similar cycloadditions under standard UV irradiation in absence of photoredox catalyst are inefficient and unselective.



SCHEME 40

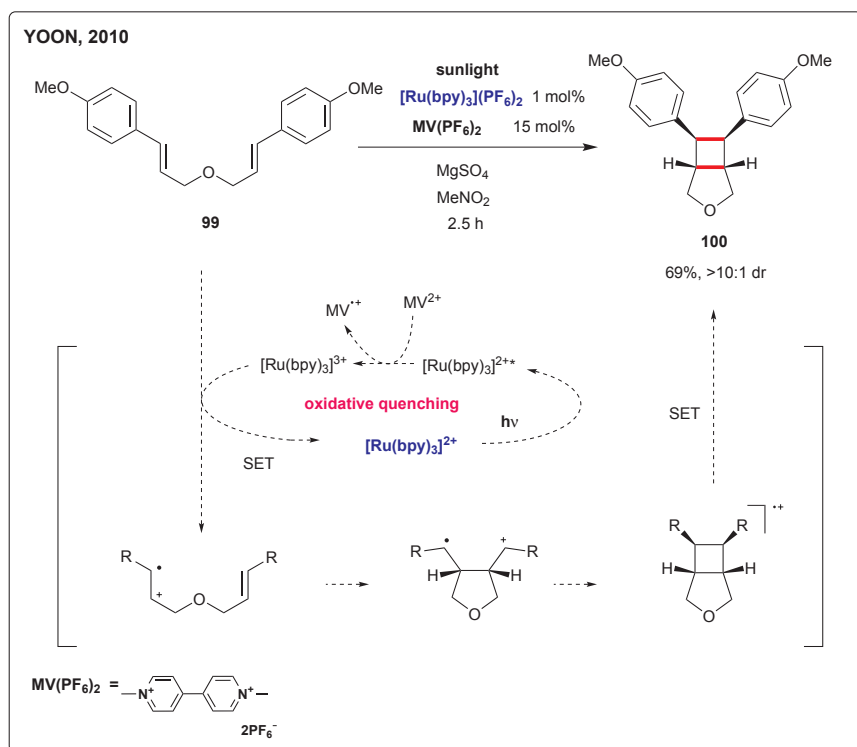
[2+2] Heterodimerizations of enones via visible-light photocatalysis (ref.<sup>57</sup>)



SCHEME 41

Selected products prepared by crossed intermolecular [2+2] cycloaddition via photoredox catalysis (ref.<sup>57</sup>)

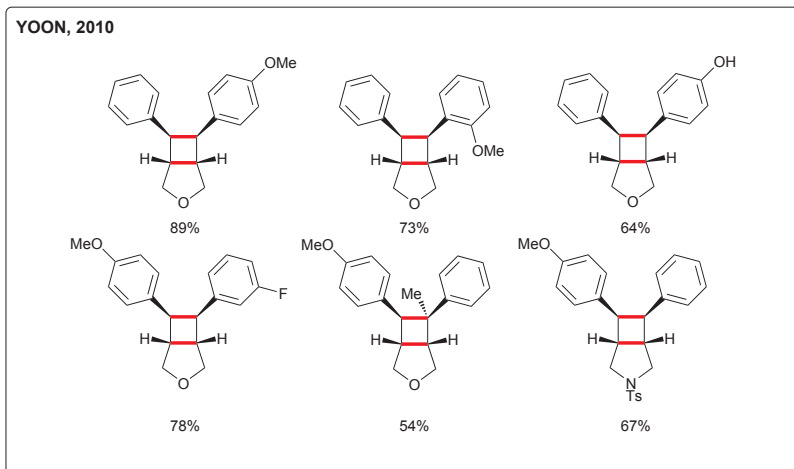
In 2010, Yoon reported [2+2] cycloadditions of electron-rich olefins (Schemes 42 and 43)<sup>58</sup> taking advantage of oxidative quenching cycle of photoexcited  $[\text{Ru}(\text{bpy})_3]^{2+*}$  state with methyl viologen ( $\text{MV}^{2+}$ ) as an electron acceptor. This process generates  $[\text{Ru}(\text{bpy})_3]^{3+}$ , a strong oxidant which is capable of oxidation of 4-methoxystyrene moiety and thus triggers a radical



SCHEME 42

Photocatalytic intramolecular [2+2] cycloaddition of an electron rich diene via oxidative quenching of photoexcited  $[\text{Ru}(\text{bpy})_3]^{2+*}$  state with methylviologen electron acceptor (ref.<sup>58</sup>)

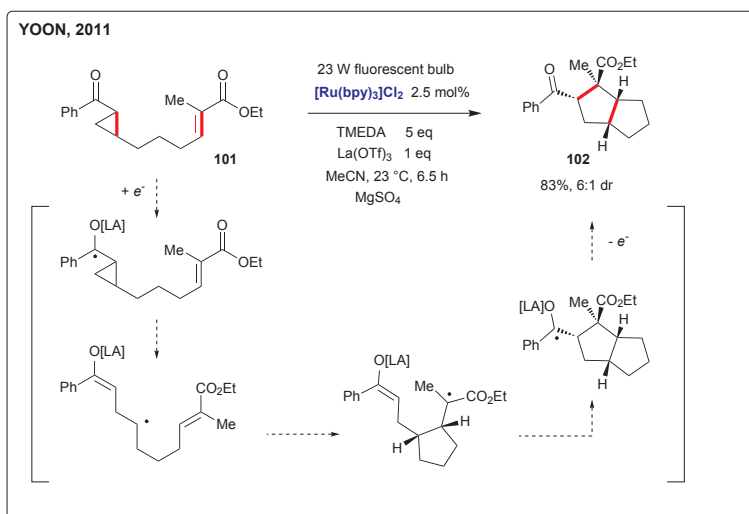
cation cyclization pathway<sup>72</sup> leading to cyclobutane structures. The electron rich diene substrates used in this work cannot be cyclized under conditions depicted in Schemes 38 and 40. Thus the reductive quenching cycle using Ru/amine (Scheme 38) and oxidative quenching cycle employing Ru/methylviologen couple (Scheme 42) are complementary strategies for [2+2] cyclization of electron poor and electron rich diene substrates, respectively.



SCHEME 43

Representative examples of photoredox [2+2] cycloadducts obtained via oxidative quenching pathway (ref.<sup>58</sup>)

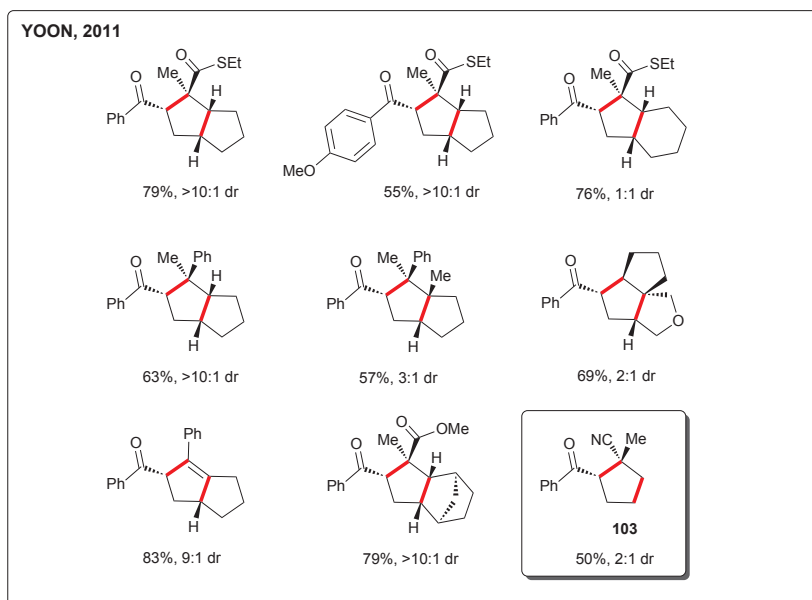
Very recently, a new method for the formal [3+2] reaction of aryl cyclopropyl ketones with olefins to afford highly substituted cyclopentane ring systems was disclosed by Yoon (Scheme 44)<sup>59</sup>. The key initiation step in



SCHEME 44

Formal [3+2] cycloaddition of aryl cyclopropyl ketone with alkene by visible-light photocatalysis (ref.<sup>59</sup>)

this transformation is the one-electron reduction of the ketone to the corresponding radical anion, which is accomplished using a photocatalytic system comprising  $[\text{Ru}(\text{bpy})_3]^{2+}$ ,  $\text{La}(\text{OTf})_3$ , and TMEDA. Notably, this method allows rapid diastereoselective construction of quaternary carbon stereocenters within a cyclopentane-containing framework. Also one intermolecular example has been established (Scheme 45, 103).

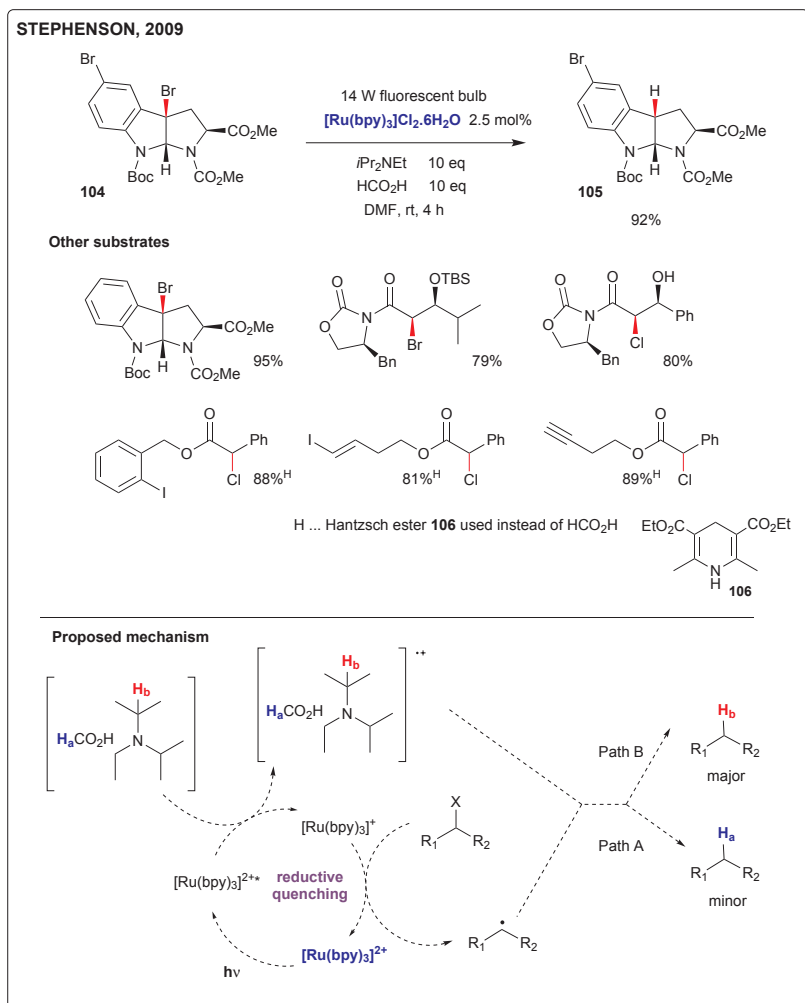


SCHEME 45

Selected products synthesized by formal [3+2] cycloaddition depicted in Scheme 44 (ref.<sup>59</sup>)

In 2009, Stephenson reported reductive dehalogenation via photoredox catalysis using  $[\text{Ru}(\text{bpy})_3]\text{Cl}_2$  in combination with *i*-Pr<sub>2</sub>NEt and HCO<sub>2</sub>H or Hantzsch ester (**106**) as the hydrogen atom donors (Scheme 46)<sup>7</sup>. Importantly, only activated C–X bonds are reduced with excellent functional-group tolerance and chemoselectivity over aryl and vinyl C–X bonds. Reductions can be accomplished on a preparative scale with as little as 0.05 mole % of the Ru catalyst. The authors proposed a mechanism involving reductive quenching pathway of the photoexcited catalyst  $[\text{Ru}(\text{bpy})_3]^{2+*}$  in which the amine serves as electron donor to generate strongly reducing  $[\text{Ru}(\text{bpy})_3]^+$ . A subsequent single-electron transfer onto the substrate generates alkyl radical, which leads to the reduced product via hydrogen atom abstraction. Based on labeling study, two concurrent plausible pathways

have been proposed (Scheme 46). Minor pathway A proceeds via hydrogen abstraction  $H_a$  from formic acid whereas majority of reduced product is generated after hydrogen abstraction  $H_b$  from the methine position of the Hünig base.

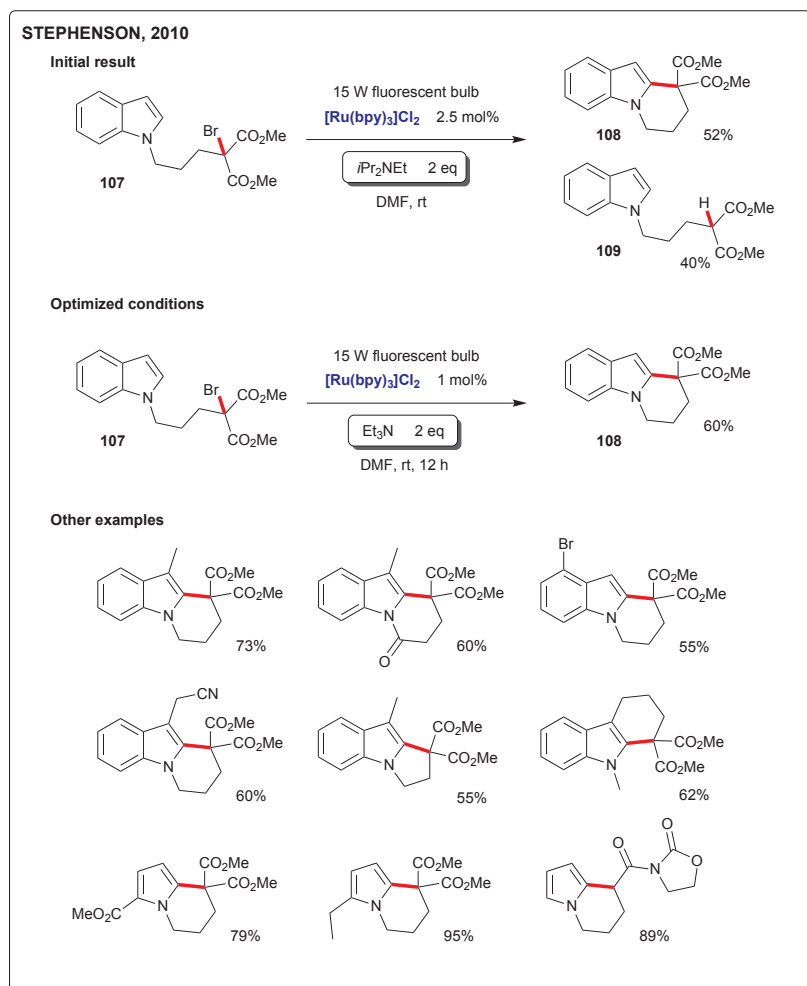


SCHEME 46

Photocatalytic reductive dehalogenation via photoredox catalysis (ref.<sup>7</sup>)

Later on, a related photoredox manifold has been explored by Stephenson for the synthesis of valuable indoles and pyrroles (Scheme 47)<sup>60</sup>. Cyclizations of structurally diverse substrates via electron transfer photo-

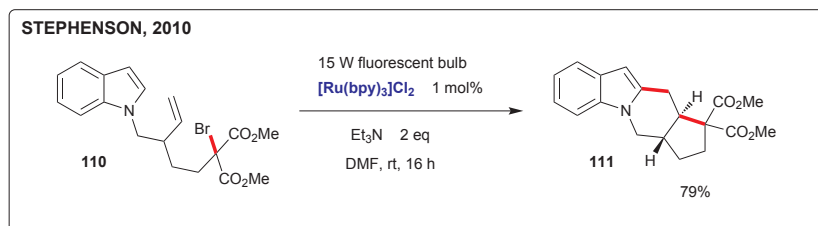
redox catalysis were triggered by  $[\text{Ru}(\text{bpy})_3]^{2+}$ /amine system. Similarly to the previous transformation depicted in Scheme 46, this process also relies on generation of radical intermediate from a C–X bond via single-electron transfer by taking advantage of the strong reductant  $[\text{Ru}(\text{bpy})_3]^+$  formed by reductive quenching pathway from  $[\text{Ru}(\text{bpy})_3]^{2+}$  and amine (Scheme 47). Malonyl radical generated this way is then intramolecularly trapped by electron rich heterocyclic system to form a new C–C bond. In this process,



SCHEME 47

Electron-transfer photoredox catalysis for intramolecular radical addition to indoles and pyrroles (ref.<sup>60</sup>)

reduced by-product **109** is formed when  $i\text{-Pr}_2\text{NEt}$  is used. However, by replacing  $i\text{-Pr}_2\text{NEt}$  with  $\text{Et}_3\text{N}$  it is possible to suppress the simple reduction pathway and enhance the desired cyclization. Apart from a broad applicability, the cascade radical cyclization has been demonstrated by the synthesis of tetracyclic compound **111** that is formed as a single diastereoisomer (Scheme 48).



SCHEME 48

Cascade radical cyclization initiated by visible-light photoredox catalysis (ref.<sup>60</sup>)

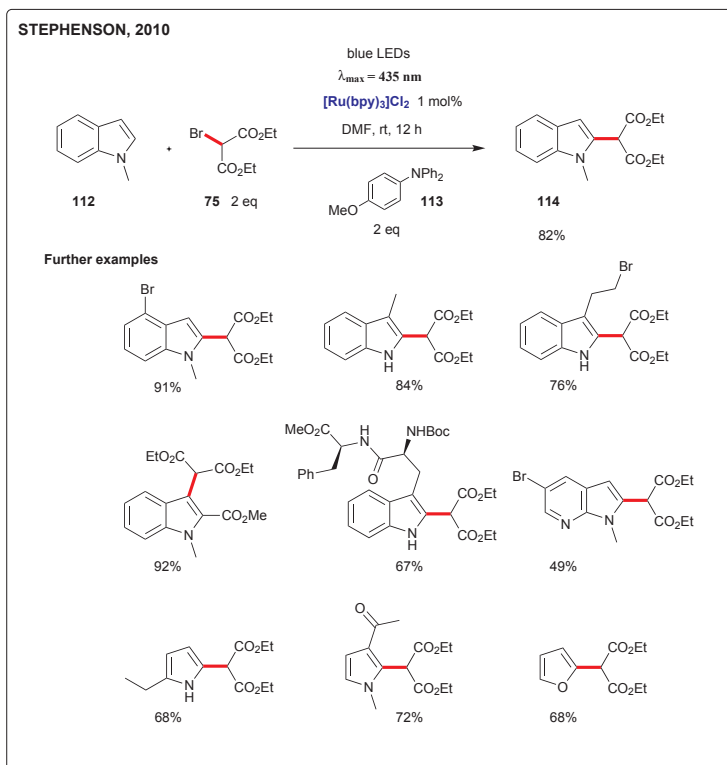
By judicious choice of the amine used, this reaction has been optimized to allow for challenging intermolecular malonation of electron-rich heterocycles with diethyl bromomalonate reagent (Schemes 49 and 50)<sup>61</sup>. Use of triethylamine instead of 4-methoxy- $N,N$ -diphenylaniline ( $\text{CH}_3\text{OC}_6\text{H}_4\text{NPh}_2$ , **113**) led to the malonylindole product **114** in only 25% yield. Light-emitting diode proved to be an advantageous source of visible light for the discussed photoredox processes. Use of 14 W fluorescent light bulb resulted in slow reactions. Thus, for example complete conversion in the transformation **112**  $\rightarrow$  **114** was reached in 5 days.

A radical cyclization onto unactivated  $\pi$ -systems, which counts as a classic free radical mediated reaction, has been initiated by photoredox catalysis under mild conditions using Ru- as well as Ir-based photocatalysts and  $\text{Et}_3\text{N}$  as a reductive quencher of the catalyst excited state (Schemes 51 and 52)<sup>62</sup>.

Gagné group disclosed recently a way to synthesize C-glycosides by addition of glycosyl halides into alkenes using visible light, an amine reductant, and  $[\text{Ru}(\text{bpy})_3](\text{BF}_4)_2$  photocatalyst (Scheme 53)<sup>67</sup>. Notably, this transformation features exclusive  $\alpha$  selectivity. The work builds on the classical free radical addition methodology pioneered by Giese<sup>73</sup> that relied on use of  $\text{Bu}_3\text{SnH}$ .

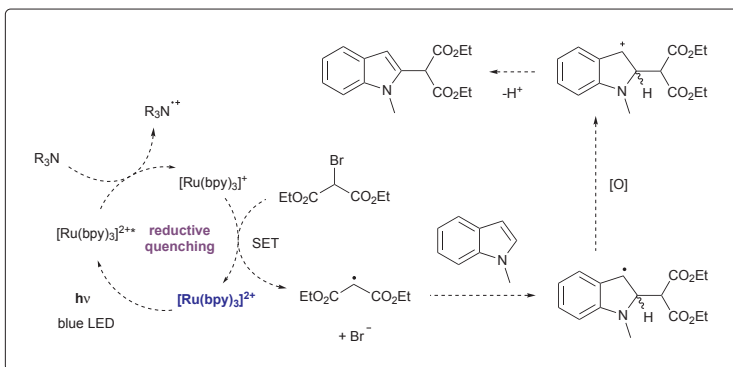
In 2010, Stephenson disclosed a protocol to effect an oxidative aza-Henry reaction. Valuable substituted amines are produced by the formation of novel C–C bond between tertiary  $N$ -arylamine and nitroalkane. The reac-





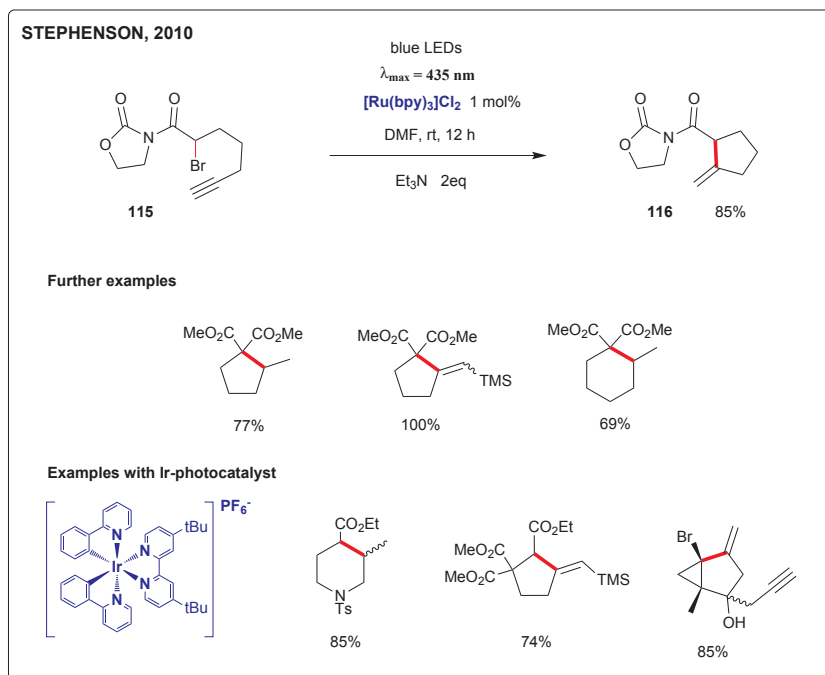
SCHEME 49

Intermolecular C–H functionalization of electron-rich heterocycles with malonate by photoredox catalysis (ref.<sup>61</sup>)



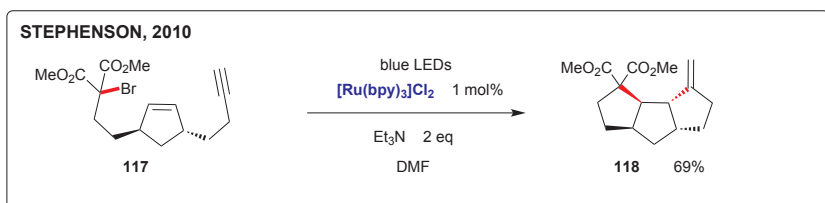
SCHEME 50

Mechanistic scheme proposed for the intermolecular radical C–H functionalization



SCHEME 51

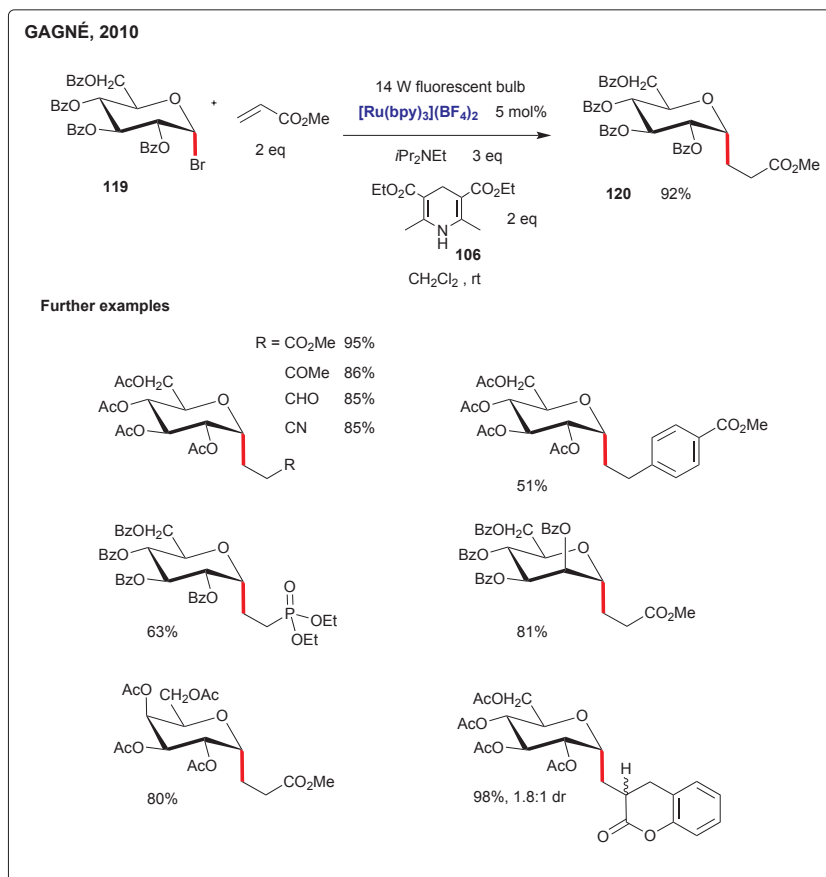
Tin-free radical cyclization with unactivated  $\pi$ -systems initiated by visible-light photoredox catalysis (ref.<sup>62</sup>)



SCHEME 52

Cascade radical cyclization with unactivated  $\pi$ -systems (ref.<sup>62</sup>)

tion is believed to proceed with intermediacy of an iminium ion generated via photoredox process (Scheme 54)<sup>63</sup>. However, at present, the identity of the oxidant leading to the key iminium intermediate is not clear. Based on the experimental evidence, adventitious atmospheric molecular oxygen has been proposed to participate in the process resulting in net acceleration of the reaction. Although [Ru(bpy)<sub>3</sub>]Cl<sub>2</sub> has been shown to catalyze the reac-

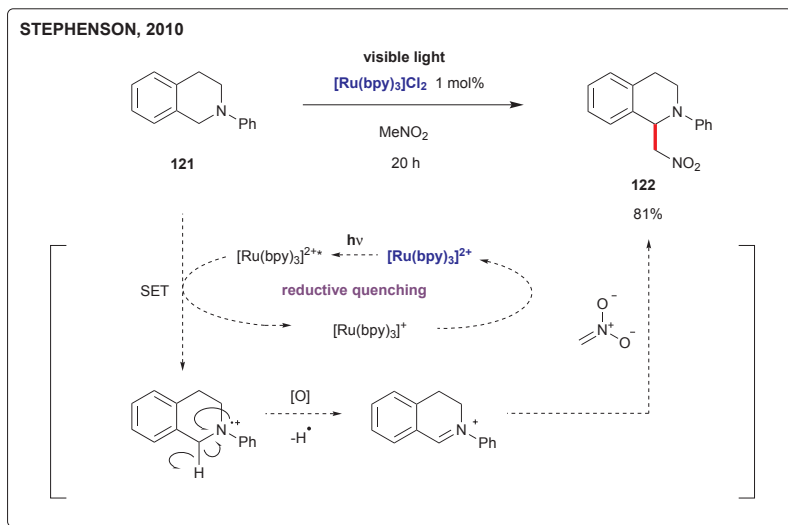


SCHEME 53

Photoredox catalysis of intermolecular addition of glycosyl halides to alkenes leading to C-glycosides with exclusive  $\alpha$  selectivity (ref.<sup>67</sup>)

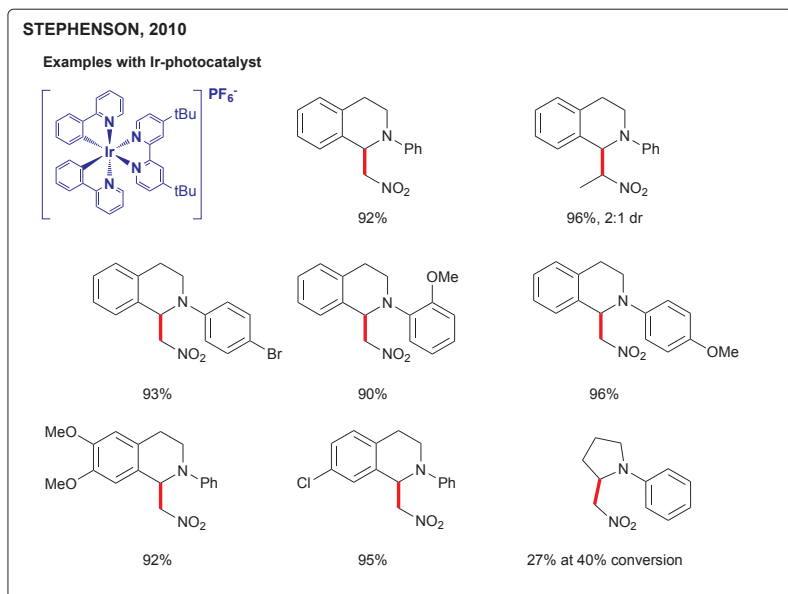
tion, Ir-based catalyst  $[\text{Ir}(\text{ppy})_2(\text{dtb-bpy})]\text{PF}_6$  is a significantly faster catalyst and therefore substrate scope of this reactions has been explored with it (Scheme 55). Mechanistic studies suggest that reductive quenching of the  $\text{Ir}^{3+}$  excited state by the tertiary amine leads to the ammonium radical cation, with subsequent catalyst turnover ( $\text{Ir}^{2+} \rightarrow \text{Ir}^{3+}$ ) likely effected by atmospheric oxygen.

Interesting example of dual catalysis has been recently reported by Rueping group (Scheme 56)<sup>68</sup>. The Mannich reaction has been triggered by combining oxidative in situ generation of iminium ion with formation of a reactive enamine nucleophile from proline and ketone. The nucleophile



SCHEME 54

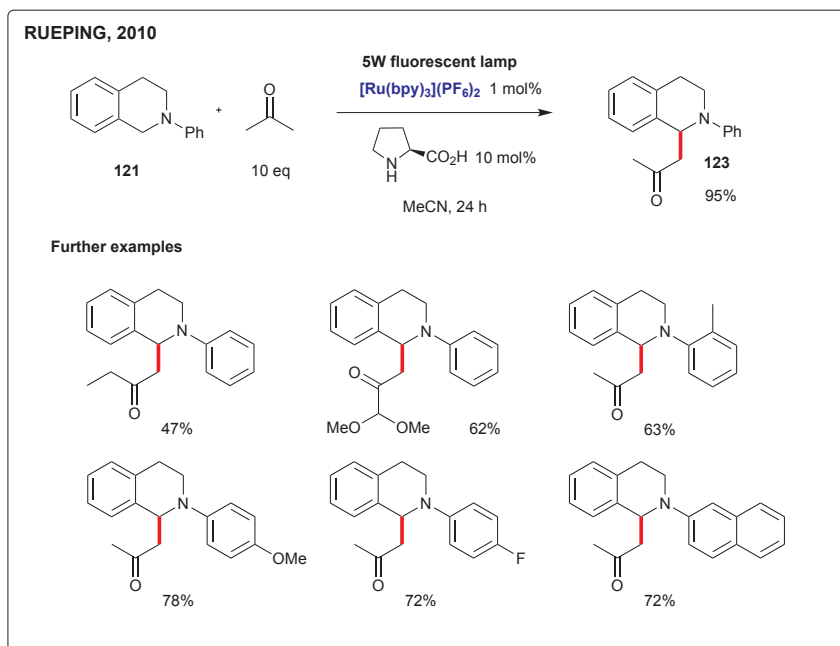
Oxidative aza-Henry reaction via visible-light photoredox catalysis with plausible mechanism (ref.<sup>63</sup>)



SCHEME 55

Products of visible-light photoredox catalysis of aza-Henry reaction with Ir-photocatalyst (ref.<sup>63</sup>)

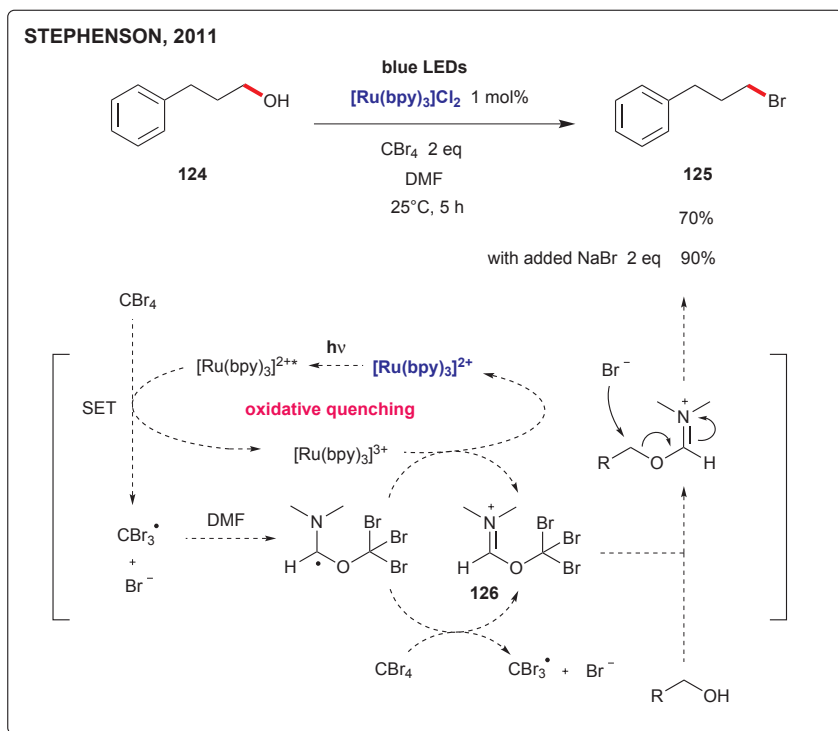
formed intercepts the iminium to afford the Mannich product. By careful choice of light source and catalyst, the reaction conditions can be tuned to match the rates of the two individual processes. In this way various tetrahydroisoquinolines (Scheme 56) can be made in a very straightforward fashion under mild reaction conditions.



SCHEME 56

Dual catalysis combining photoredox and Lewis base catalysis for direct Mannich reactions (ref.<sup>68</sup>)

In a recent publication, Stephenson group described a useful photocatalytic variant of the venerable Appel reaction (Scheme 57)<sup>64</sup>. In this photocatalytic halogenation, alcohols are converted to bromides or iodides ( $\text{R-OH} \rightarrow \text{R-X}$ ) using DMF,  $[\text{Ru}(\text{bpy})_3]\text{Cl}_2$  catalyst, and  $\text{CBr}_4$  or  $\text{CHI}_3$ . Addition of 2 equivalents of  $\text{NaBr}$  substantially improved the yield in the model reaction. Notably, this transformation involves DMF playing a crucial role in the alcohol activation ( $\text{R-OH}$ ) as has been revealed by isolation of the corresponding formate esters  $\text{R-OCHO}$  after early quenching of the reacting mixture. The authors proposed oxidative quenching of  $[\text{Ru}(\text{bpy})_3]^{2+*}$  by  $\text{CBr}_4$ , leading to  $\text{CBr}_3^{\bullet}$  and subsequently to the iminium species **126** that

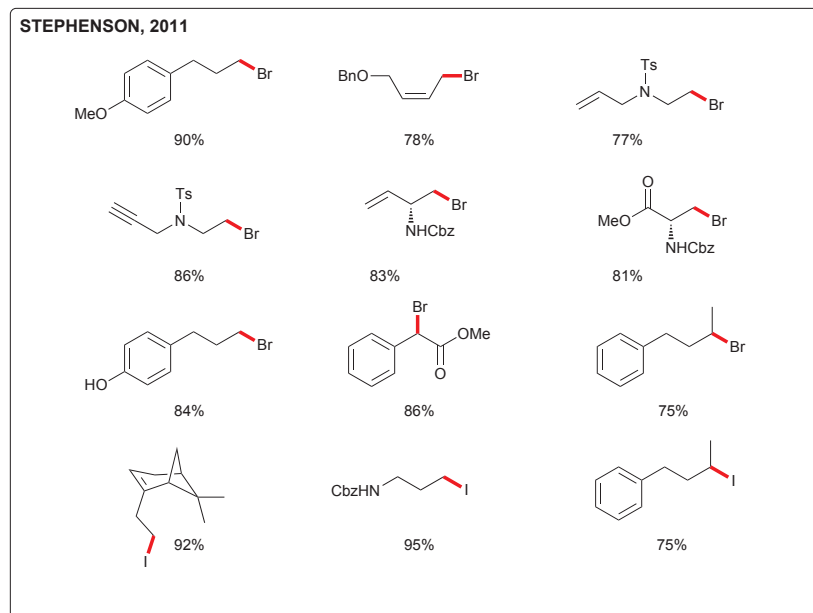


SCHEME 57

Halogenation of alcohols via visible-light photoredox catalysis (ref.<sup>64</sup>)

leads to the alcohol activation (Scheme 57). As compared to the original Appel reaction<sup>74</sup>, this photocatalytic version is substantially more atom-economic obviating the use of stoichiometric triphenylphosphine reductant and avoiding disposal of its unpleasant oxidation product triphenylphosphine oxide. Functional group tolerance (Scheme 58) and mild conditions make this new photocatalytic alkylhalide synthesis an attractive alternative to the other established protocols used to convert alcohols to halides.

Most recently, Stephenson group disclosed a related oxidative quenching pathway to effect atom transfer radical addition (ATRA) of haloalkanes to olefins<sup>65a</sup>. The reaction is efficiently performed with the  $[\text{Ir}(\text{dF}(\text{CF}_3)\text{ppy})_2\text{-(dtb-bpy)}]\text{PF}_6$  photocatalyst. Furthermore, oxidation of electron rich arenes resulting in the selective deprotection of *para*-methoxybenzyl (PMB) ethers has been reported<sup>65b</sup>. Similarly to the ATRA, in this reaction too, oxidative quenching cycle of the Ir photocatalyst is effected by using haloalkanes such as  $\text{BrCCl}_3$ .



SCHEME 58

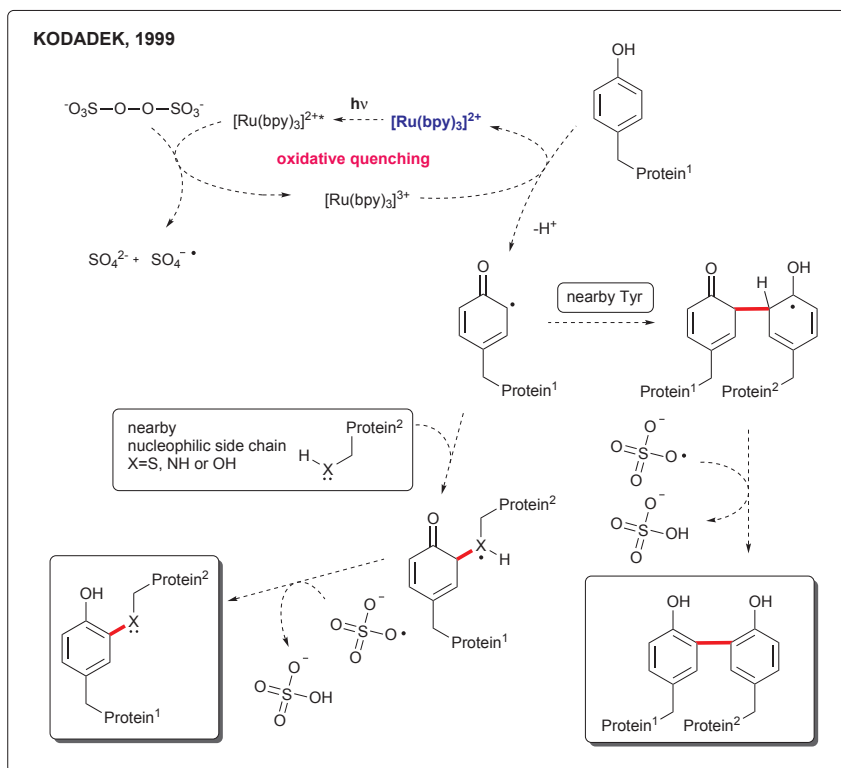
Examples of products of photocatalytic phosphine-free halogenation of alcohols (ref.<sup>64</sup>)

## 5. PHOTOREDOX CHEMISTRY AS A TOOL FOR MAKING AND BREAKING BONDS IN CHEMICAL BIOLOGY AND MATERIALS CHEMISTRY

### 5.1 Chemical Biology

In a seminal paper from 1999, Kodadek group introduced  $[\text{Ru}(\text{bpy})_3]^{2+}$  photocatalyst as new tool for chemical biology. Specifically, oxidative quenching pathway of  $[\text{Ru}(\text{bpy})_3]^{2+*}$  has been taken advantage of to effect a very rapid and efficient protein cross-linking (Scheme 59)<sup>75a</sup>. Ammonium persulfate was used as an oxidative quencher to generate  $[\text{Ru}(\text{bpy})_3]^{3+}$  as a potent one-electron oxidant. It has been proposed that this strongly oxidizing species, generated in situ using visible-light excitation, can oxidize tyrosine moieties in proteins. The resultant radical was suggested to cross-link two associated proteins by at least two mechanisms depicted in Scheme 59. In case another tyrosine residue is in proximity, aryl–aryl bond formation can take place. Alternatively, a nucleophilic lysine or cysteine group can attack the phenol radical to afford a new heteroatom–arene bond. In both pathways, a hydrogen atom is lost to form stable products,

and the sulfate radical produced during Ru(III) formation was proposed to play a key role in this step. Very high yields of cross-linked products were reported with irradiation times of less than 1 s. Later study on this photo-induced cross-linking of proteins revealed more details about the scope, limitations, and mechanistic aspects<sup>75b</sup>. This method was shown to be useful for quantitative characterization of protein–protein and protein–peptide complexes<sup>76</sup>.



SCHEME 59

Phototriggered protein cross-linking using photoredox manifold of  $[\text{Ru}(\text{bpy})_3]^{2+}$  in conjunction with persulfate oxidative quencher (ref.<sup>75</sup>)

Notably, chemical principle of Kodadek method of making dityrosine linkages is similar to that of Ohkubo method for synthesis of BINOL from 2-naphthol (cf. Schemes 59 and 21). Both methods utilize oxidative quenching cycle of  $\text{Ru}^{2+*}$  complex leading to generation of reactive phenol radical from phenolic substrate.



Kodadek group also used  $[\text{Ru}(\text{bpy})_3]^{2+}$  warheads in chromophore-assisted light inactivation (CALI) of proteins<sup>77</sup>.  $[\text{Ru}(\text{bpy})_3]^{2+}$  moiety was shown to work as a competent chromophore for singlet oxygen generation, which is able to inactivate target proteins. A specific and unusually efficient inactivation of a biological target with  $[\text{Ru}(\text{bpy})_3]^{2+}$  constructs is due to a local release of very reactive singlet oxygen that takes place on the ruthenium warhead in the direct proximity of the target protein. In this context, the performance of  $[\text{Ru}(\text{bpy})_3]^{2+}$  was found superior to the most common organic sensitizers such as fluorescein that has been employed as a warhead in the initial CALI experiments. In 2010, this attractive strategy was used to transform modest protein binders into much more potent inhibitors without lengthy compound optimization<sup>78</sup>. The only step required is to attach the  $[\text{Ru}(\text{bpy})_3]^{2+}$  warhead to the protein binder of interest. To this end, synthetic peptoid- $[\text{Ru}(\text{bpy})_3]^{2+}$  conjugates were designed to bind to proteins, resulting in highly potent and specific inactivation of the target protein triggered by singlet oxygen production upon irradiation with visible light.

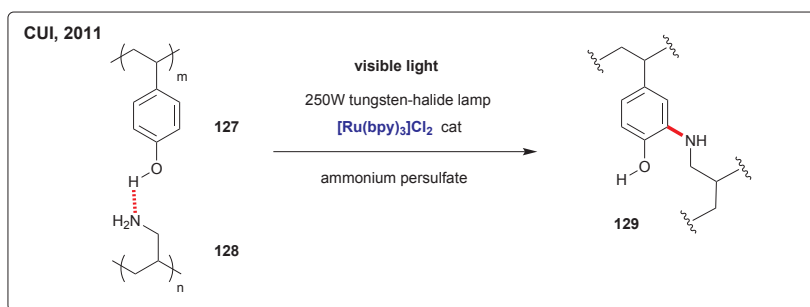
In general, biological applications of photoredox complexes related to  $[\text{Ru}(\text{bpy})_3]^{2+}$  are in focus of trully fascinating research endeavors with promising future. As the more extensive coverage of this territory is beyond the scope of this review, the interested readers are referred to excellent reviews summarizing the status and challenges in the area<sup>79</sup>.

## 5.2 Materials Chemistry

In 2005, light-activated  $[\text{Ru}(\text{bpy})_3]^{2+}$ /persulfate combination discussed in conjunction with Scheme 59 has been used by Elvin group to form dityrosine cross-links in natural rec1-resilin. This procedure led to rapid, quantitative and controllable formation of very high molecular weight rubber-like polymeric biomaterial<sup>80</sup>. Other interesting photoredox cross-linked materials generated from tyrosine-rich protein precursors, such as fibrinogen, have been disclosed recently by Elvin<sup>81</sup> and Tranquillo<sup>82</sup> groups. Because of their superior mechanical properties, Elvin proposed use of these biomaterials in various surgical applications.

Visible light-triggered chemical cross-linking has been recently reported for facile preparation of microgels<sup>83</sup> with interesting stability. Phenol groups grafted on sodium alginate give rise to novel bonds that are similar to the dityrosine linkages discussed above. Applications of this biocompatible and biodegradable microgel in biology have been proposed. Cui group has also utilized related cross-linking strategy as a method to fabricate robust multilayer films by forming bonds between primary amine groups and

phenol moieties<sup>84</sup>. Visible-light irradiation of hydrogen-bonded layers of poly(allylamine) and poly(4-vinylphenol) led to formation of highly stable covalent –Ar–NH– interlayer bonds (e.g. **127** + **128** → **129**, Scheme 60). Solid-state <sup>13</sup>C NMR, FT-IR, and N 1s XPS spectra were used to confirm the formation of new C–N bonds on the aromatic rings. Thus, layer-by-layer self-assembled polymer composed of 15-bilayers was made significantly more corrosion-resistant by photoredox cross-linking as compared to the native non-cross-linked polymer film. All the discussed bond formations relying on oxidizable phenol moiety are based on oxidative quenching pathway of [Ru(bpy)<sub>3</sub>]<sup>2+\*</sup> generating strongly oxidizing [Ru(bpy)<sub>3</sub>]<sup>3+</sup> species giving rise to the reactive phenol radical as outlined in Scheme 59.

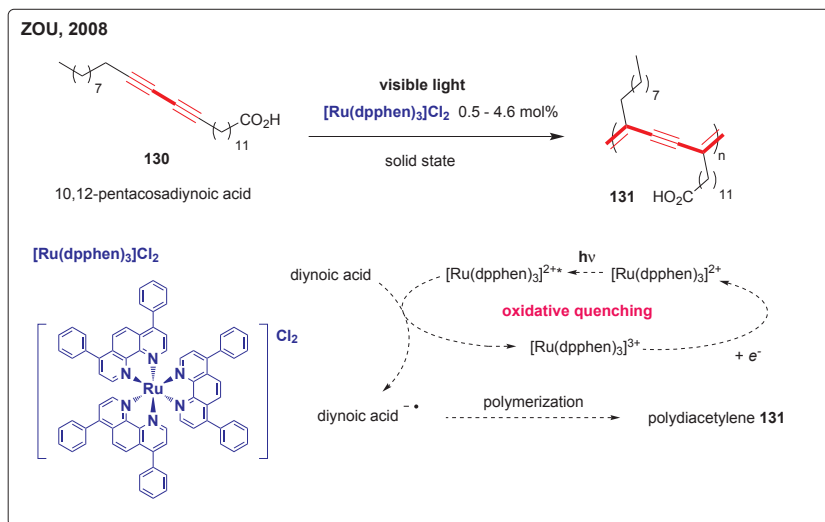


SCHEME 60

Hydrogen-bonding directed chemical cross-linking using visible-light photoredox manifold of [Ru(bpy)<sub>3</sub>]<sup>2+</sup> and reactivity of phenol moieties in the presence amine nucleophiles (ref.<sup>84</sup>)

In 2008, Zou group described solid-state polymerization of diacetylene monomers initiated by [Ru(dpphen)<sub>3</sub>]<sup>2+</sup> and visible light. Embedding of the photocatalyst into the hybrid films of the diacetylene monomer led after visible-light irradiation to polydiacetylene conjugated polymer **131** (Scheme 61)<sup>85</sup>. The mechanism of the photoinitiation is discussed, and an explanation based on photoinduced electron transfer from excited state of [Ru(dpphen)<sub>3</sub>]<sup>2+</sup> to diacetylene moiety of the 10,12-pentacosadiynoic acid (**130**) monomer has been suggested (Scheme 61). Recently, polymerization of epoxides involving [Ru(bpy)<sub>3</sub>]<sup>2+</sup> photocatalyst has been disclosed by Lalevée group<sup>86</sup>. This fast transformation relies on photoinitiation system composed of [Ru(bpy)<sub>3</sub>]<sup>2+</sup>, Ph<sub>2</sub>I<sup>+</sup>, and (TMS)<sub>3</sub>SiH additive.

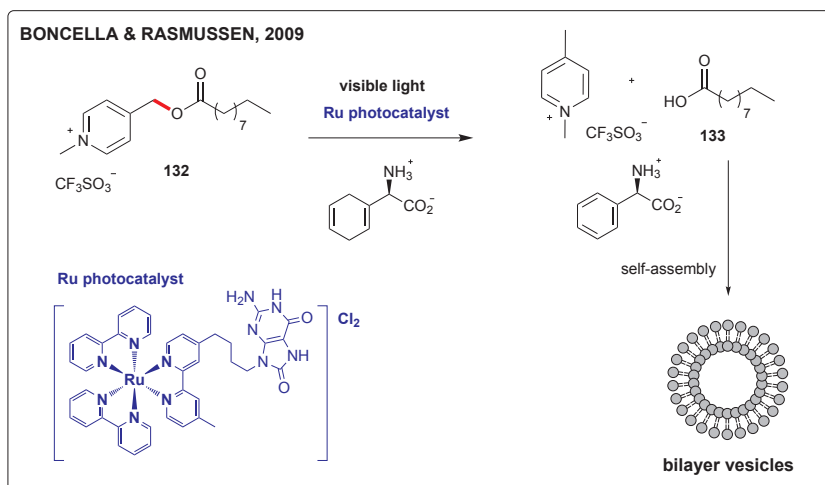
Recently, photoredox manifold of [Ru(bpy)<sub>3</sub>]<sup>2+</sup> complexes has been used to effect release of carboxylic acids from their *N*-methyl-4-picolinium esters (Schemes 62 and 64)<sup>87,88</sup>. In their report, Boncella, Rasmussen, and coworkers showed that decanoic acid **133** can be released from its *N*-methyl-



SCHEME 61

Ruthenium(II) complex-sensitized solid-state polymerization of diacetylene monomer (ref.<sup>85</sup>)

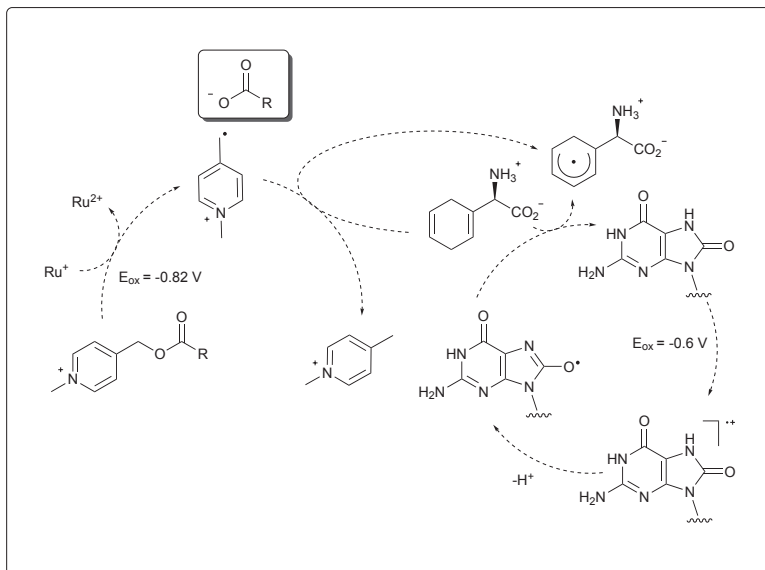
4-picolinium ester **132** by irradiation in presence of [8-oxo-G-Ru(bpy)<sub>3</sub>]<sup>2+</sup> photocatalysts (Schemes 62)<sup>87</sup>. After the photoinitiated bond scission and release of the free fatty acid, spontaneous formation of bilayer assemblies



SCHEME 62

Nucleobase mediated photocatalytic vesicle formation by release of decanoic acid from its picolinium ester (ref.<sup>87</sup>)

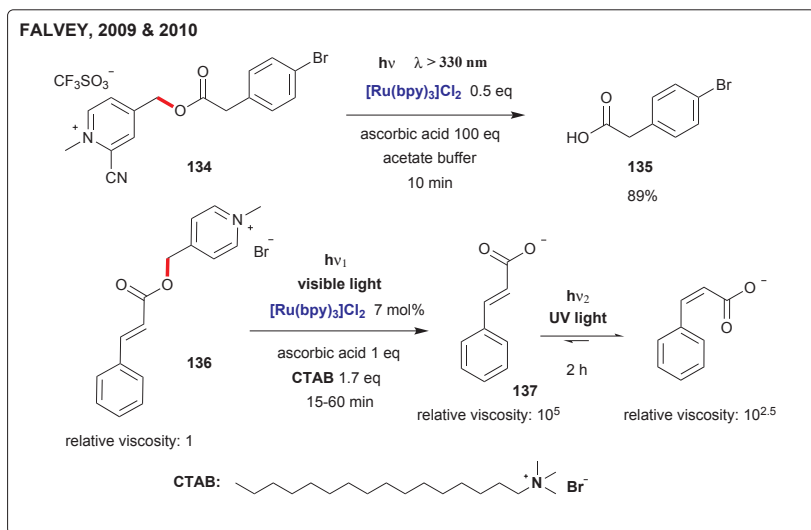
such as vesicles was observed. This is a conceptually interesting example of triggering self-assembly of compartmentalized bilayer system from a homogeneous precursor mixture. Because it is very easily oxidized, 8-oxoguanine moiety has been selected for attachment to the photoredox active  $[\text{Ru}(\text{bpy})_3]^{2+}$  center. It can be oxidized even more readily than the most easily oxidized conventional nucleobase guanine. In this context, 8-oxo-G moiety has been proposed to serve as a sufficiently strong electron donor to provide an electron to reductively quench the excited state of the  $\text{Ru}^{2+}$  core of the photocatalyst resulting in strongly reducing  $\text{Ru}^+$  species. The  $\text{Ru}^+$  reductant then transfers its electron onto the *N*-methyl-4-picolinium moiety of the ester which in turn leads to the release of the free acid **133** (Scheme 63). Notably, when 8-oxoguanine moiety was replaced by simple guanine, the catalytic system led only to mediocre production of the free decanoic acid as indicated by the NMR study.



SCHEME 63

Proposed mechanistic pathway of nucleobase mediated photocatalytic release of carboxylic acid from its ester precursor

Recently, Falvey group studied photodeprotection of 2-cyano-4-picolinium esters to release free carboxylic acids (e.g. **134**  $\rightarrow$  **135**, Scheme 64)<sup>88</sup>. By taking advantage of ascorbic acid as the water soluble reductant, they triggered reductive quenching pathway of excited state  $[\text{Ru}(\text{bpy})_3]^{2+*}$  photocatalyst in an aqueous system.



SCHEME 64  
Photocatalytic cleavage of picolinium esters (refs<sup>88,89</sup>)

In a related publication, by using visible-light photodeprotection **136** → **137** in the environment of aqueous solution of cationic surfactant cetyltrimethylammonium bromide (CTAB), viscosity of the solution has been shown to increase significantly by a factor of ca.  $10^5$  (Scheme 64)<sup>89</sup>. This dramatic change of the liquid physical properties has been ascribed to a formation of long entangled wormlike micelles resulting from a combination of photoreleased *trans*-cinnamate anions **137** with cationic surfactant CTAB. Remarkably, the follow-up UV irradiation can be used to attenuate the viscosity by *cis-trans* isomerization of the cinnamate double bond. With this bi-modal photocontrol, the authors introduced a new concept to influence the aqueous solution viscosity by orthogonal use of visible light and UV light. The potential use of this phenomenon in biological and materials applications has been proposed<sup>90</sup>.

## 6. CONCLUSIONS AND OUTLOOK

Since 2008, the field of visible-light photoredox catalysis for organic synthesis has emerged as a very prolific area of research. It is anticipated that it will have profound impact on preparative organic chemistry in the future. The current wave of interest is due to the major seminal studies by MacMillan, Yoon, and Stephenson groups. Before the fast acceleration in

this branch during the last three years, the limited number of scattered examples relevant to organic synthesis remained dormant in the literature. However, now, the early attempts published in the 20th century might serve as an inspiration for the field, which is on the rise. Therefore, awareness of the pioneering efforts by groups of Kellogg, Pac, Willner, Deronzier, Tanaka, Tomioka, Fukuzumi, Okada and Oda, Ohkubo, Barton, and Kodadek may help to nurture the current formative era and conceptual expansion of this branch of photocatalysis.

In 2010, the essence and promise of research into photoredox catalysis with visible light has been nicely summarized by Yoon: *“The versatility of  $[Ru(bpy)_3]^{2+}$  arises from the ability to access either photooxidative or photoreductive reactivity by choosing the appropriate oxidative and reductive quencher, respectively (see Scheme 2 in this review). In both regimes, the photophysical properties of  $[Ru(bpy)_3]^{2+}$  enable a variety of inexpensive, readily available sources of visible light to be utilized, including sunlight. In addition, there exists a vast wealth of electrochemical literature that describes synthetically useful organic transformations initiated by one-electron redox processes. It is expected that photocatalytic systems exploiting the reactivity of  $[Ru(bpy)_3]^{2+}$  should also be able to efficiently promote similar reactivity”*<sup>58</sup>. Likewise, it can be anticipated that photoredox reactivity of complexes based on metals other than Ru (e.g. Ir<sup>91</sup>, Re<sup>92,93</sup>, and bimetallic photocatalysts<sup>94</sup>) will also be intensively explored, as indicated by the current shift of interest to Ir photocatalysts in the recent work of MacMillan<sup>55,56</sup> and Stephenson<sup>62,63,65</sup>. Additionally, transformations triggered by purely organic photoredox catalysts start to attract attention as highlighted in the report by Zeitler group<sup>8,95</sup>. In general, it is eminent that many interesting and useful tools for molecule makers will arise from this exciting area of research during the 21st century<sup>96</sup>.

## 7. ABBREVIATIONS

acac	acetylacetonato
ATRA	atom transfer radical addition
BINOL	1,1'-bi-2-naphthol
BNAH	1-benzyl-1,4-dihydronicotinamide
bpy	2,2'-bipyridine
CTAB	cetyltrimethylammonium bromide
dF(CF <sub>3</sub> )ppy	2-(2,4-difluorophenyl)-5-trifluoromethylpyridinato-C6,N
dpphen	4,7-diphenyl-1,10-phenanthroline
dtb-bpy	4,4'-di- <i>tert</i> -butyl-2,2'-bipyridine
EDTA	ethylenediaminetetraacetic acid
menbpy	4,4'-di(1 <i>R</i> ,2 <i>S</i> ,5 <i>R</i> )-(-)-menthoxycarbonyl-2,2'-bipyridine
MLCT	metal-to-ligand charge transfer

NADH	nicotinamide adenine dinucleotide
PMB	<i>para</i> -methoxybenzyl
ppy	2-phenylpyridinato-C <sub>2</sub> ,N
SET	single-electron transfer
TEOA	triethanolamine, tris(2-hydroxyethyl)amine

The author would like to thank Dr. U. Jahn of the Institute for stimulating and helpful discussions. This work was supported by the Czech Science Foundation (Grant No. P207/10/2391) and by the Institute of Organic Chemistry and Biochemistry, Academy of Sciences of the Czech Republic, v.v.i. (Z4 055 0506).

## 8. REFERENCES AND NOTES

1. For a visionary address on the future of photochemistry, see: a) Ciamician G.: *Science* **1912**, 36, 385; For excellent discussion on the beginnings of organic photochemistry, see: b) Roth H. D.: *Angew. Chem., Int. Ed. Engl.* **1989**, 28, 1193.
2. a) Klán P., Wirz J.: *Photochemistry of Organic Compounds: From Concepts to Practice*. Wiley, Chichester 2009; b) Turro N. J., Ramamurthy V., Scaiano J. C.: *Modern Molecular Photochemistry of Organic Molecules*. University Science Books, Sausalito/elfassembled 2010.
3. For selected reviews on photocatalytic formation of important bonds in organic chemistry, see: a) Fagnoni M., Dondi D., Ravelli D., Albini, A.: *Chem. Rev.* **2007**, 107, 2725; b) Hoffmann N.: *Chem. Rev.* **2008**, 108, 1052; c) Svoboda J., König B.: *Chem. Rev.* **2006**, 106, 5413; d) Bach T.: *Synthesis* **1998**, 683; For photochemical synthesis of fine chemicals with sunlight, see: e) Esser P., Pohlmann B., Scharf H.-D.: *Angew. Chem., Int. Ed. Engl.* **1994**, 33, 2009.
4. For reviews on photoredox catalysis with visible light, see: a) Narayanam J. M. R., Stephenson C. R. J.: *Chem. Soc. Rev.* **2011**, 40, 102; b) Yoon T. P., Ischay M. A., Du J.: *Nat. Chem.* **2010**, 2, 527; c) Zeitler K.: *Angew. Chem. Int. Ed.* **2009**, 48, 9785; d) Renaud P., Leong P.: *Science* **2008**, 322, 55.
5. Nicewicz D. A., MacMillan D. W. C.: *Science* **2008**, 322, 77.
6. Ischay M. A., Anzovino M. E., Du J., Yoon T. P.: *J. Am. Chem. Soc.* **2008**, 130, 12886.
7. Narayanam J. M. R., Tucker J. W., Stephenson C. R. J.: *J. Am. Chem. Soc.* **2009**, 131, 8756.
8. Neumann M., Földner S., König B., Zeitler K.: *Angew. Chem. Int. Ed.* **2011**, 50, 951.
9. Burstall F. H.: *J. Chem. Soc.* **1936**, 173.
10. Interestingly high configurational stability of [Ru(bpy)<sub>3</sub>]<sup>2+</sup> was in stark contrast to analogous iron and nickel complexes studied previously by Blau and Werner: a) Blau F.: *Monatsh. Chem.* **1898**, 19, 647; b) Werner A.: *Chem. Ber.* **1912**, 45, 433; For configurationally stable octahedral iron complexes, see: c) Monchaud D., Jodry J. J., Pomeranc D., Heitz V., Chambron J. C., Sauvage J. P., Lacour J.: *Angew. Chem. Int. Ed.* **2002**, 41, 2317, and references therein.
11. a) Sabbatini N., Balzani V.: *J. Am. Chem. Soc.* **1972**, 94, 7587; b) Gafney H. D., Adamson A. W.: *J. Am. Chem. Soc.* **1972**, 94, 8238; c) Wrighton M., Markham J.: *J. Phys. Chem.* **1973**, 77, 3042; d) Bock C. R., Meyer T. J., Whitten D. G.: *J. Am. Chem. Soc.* **1974**, 96, 4710; e) Navon G., Sutin N.: *Inorg. Chem.* **1974**, 13, 2159.

12. For reviews, see: a) Campagna S., Puntoriero F., Nastasi F., Bergamini G., Balzani V.: *Top. Curr. Chem.* **2007**, 280, 117; b) Juris A., Balzani V., Barigelletti F., Campagna S., Belser P., von Zelewsky A.: *Coord. Chem. Rev.* **1988**, 84, 85; c) Kalyanasundaram K.: *Coord. Chem. Rev.* **1982**, 46, 159; d) Sutin N.: *J. Photochem.* **1979**, 10, 19; e) Whitten D. G.: *Acc. Chem. Res.* **1980**, 13, 83.
13. a) Kalyanasundaram K., Kiwi J., Gratzel M.: *Helv. Chim. Acta* **1978**, 61, 2720; b) Gratzel M., Kiwi J.: *J. Am. Chem. Soc.* **1979**, 101, 7214.
14. a) Creutz C., Sutin N.: *Proc. Natl. Acad. Sci. U.S.A.* **1975**, 72, 2858; For recent reviews on utilization of solar energy, see: b) Lewis N. S., Nocera D. G.: *Proc. Natl. Acad. Sci. U.S.A.* **2006**, 103, 15729; c) Balzani V., Credi A., Venturi M.: *ChemSusChem* **2008**, 1, 26; For excellent overviews on various relevant environmental issues, see: d) Armaroli N., Balzani V.: *Chem. Asian J.* **2011**, 6, 768; e) Jenck J. F., Agterberg F., Droescher M. J.: *Green Chem.* **2004**, 6, 544.
15. Ceroni P., Bergamini G., Balzani V.: *Angew. Chem. Int. Ed.* **2009**, 48, 8516.
16. Hedstrand D. M., Kruizinga W. H., Kellogg R. M.: *Tetrahedron Lett.* **1978**, 19, 1255.
17. van Bergen T. J., Hedstrand D. M., Kruizinga W. H., Kellogg R. M.: *J. Org. Chem.* **1979**, 44, 4953.
18. Mashraqui S. H., Kellogg R. M.: *Tetrahedron Lett.* **1985**, 26, 1453.
19. Pac C., Ihama M., Yasuda M., Miyauchi Y., Sakurai H.: *J. Am. Chem. Soc.* **1981**, 103, 6495.
20. Pac C., Miyauchi Y., Ishitani O., Ihama M., Yasuda M., Sakurai H.: *J. Org. Chem.* **1984**, 49, 26.
21. Ishitani O., Pac C., Sakurai H.: *J. Org. Chem.* **1983**, 48, 2941.
22. Ishitani O., Yanagida S., Takamuku S., Pac C.: *J. Org. Chem.* **1987**, 52, 2790.
23. Maidan R., Goren Z., Becker J. Y., Willner I.: *J. Am. Chem. Soc.* **1984**, 106, 6217.
24. Goren Z., Willner I.: *J. Am. Chem. Soc.* **1983**, 105, 7764.
25. Willner I., Goren Z., Mandler D., Maidan R., Degani Y.: *J. Photochem.* **1985**, 28, 215.
26. Maidan R., Willner I.: *J. Am. Chem. Soc.* **1986**, 107, 1080.
27. For a related example, see: Mandler D., Willner I.: *J. Am. Chem. Soc.* **1984**, 106, 5352.
28. Willner I., Tsfania T., Eichen Y.: *J. Org. Chem.* **1990**, 55, 2656.
29. Tomioka H., Ueda K., Ohi H., Izawa Y.: *Chem. Lett.* **1986**, 1359.
30. Cano-Yelo H., Deronzier A.: *J. Chem. Soc., Perkin Trans. 2* **1984**, 1093.
31. Oxidative quenching of  $[\text{Ru}(\text{bpy})_3]^{2+}$  with  $p\text{-RC}_6\text{H}_4\text{N}_2^+$  has been also studied in the context of two-compartment photoelectrochemical cells, see: Cano-Yelo H., Deronzier A.: *J. Chem. Soc., Faraday Trans. 1* **1984**, 80, 3011.
32. Cano-Yelo H., Deronzier A.: *Tetrahedron Lett.* **1984**, 25, 5517.
33. Cano-Yelo H., Deronzier A.: *New J. Chem.* **1987**, 11, 479.
34. Hironaka K., Fukuzumi S., Tanaka T.: *J. Chem. Soc., Perkin Trans. 2* **1984**, 1705.
35. a) Rakshys J. W., Jr.: *Tetrahedron Lett.* **1971**, 4745; b) Bank S., Bank J. F.: *Tetrahedron Lett.* **1969**, 4533; c) Kern J. M., Sauvage J. P.: *J. Chem. Soc., Chem. Commun.* **1987**, 546.
36. Fukuzumi S., Mochizuki S., Tanaka T.: *J. Phys. Chem.* **1990**, 94, 722.
37. For the initial study on acid catalysis in photoinduced electron transfer from  $[\text{Ru}(\text{bpy})_3]^{2+}$  to substituted acetophenones, see: a) Fukuzumi S., Ishikawa K., Hironaka K., Tanaka T.: *J. Chem. Soc., Perkin Trans. 2* **1987**, 751; For a related study with ferrocene reductants in their ground state, see: b) Fukuzumi S., Mochizuki S., Tanaka T.: *J. Am. Chem. Soc.* **1989**, 111, 1497.
38. Okada K., Okamoto K., Morita N., Okubo K., Oda M.: *J. Am. Chem. Soc.* **1991**, 113, 9401.



39. Okada K., Okubo K., Morita N., Oda M.: *Tetrahedron Lett.* **1992**, 33, 7377.
40. Okada K., Okubo K., Morita N., Oda M.: *Chem. Lett.* **1993**, 2021.
41. Barton D. H. R., Csiba M. A., Jaszberenyi J. C.: *Tetrahedron Lett.* **1994**, 35, 2869.
42. Hamada T., Ishida H., Usui S., Watanabe Y., Tsumura K., Ohkubo K.: *J. Chem. Soc., Chem. Commun.* **1993**, 909.
43. Hamada T., Ishida H., Usui S., Tsumura K., Ohkubo K.: *J. Mol. Catal.* **1994**, 88, L1.
44. Ohkubo K., Hamada T., Ishida H.: *J. Chem. Soc., Chem. Commun.* **1993**, 1423.
45. Ohkubo K., Watanabe M., Ohta H., Usui S.: *J. Photochem. Photobiol., A* **1996**, 95, 231.
46. a) Rau H.: *Chem. Rev.* **1983**, 83, 535; b) Inoue Y.: *Chem. Rev.* **1992**, 92, 741.
47. Irie R., Masutani K., Katsuki T.: *Synlett* **2000**, 1433.
48. For recent advances in asymmetric oxidative coupling of 2-naphthol and its derivatives, see: a) Wang H.: *Chirality* **2010**, 22, 827; For further review, see: b) Giri R., Shi B. F., Engle K. M., Maugel N., Yu J. Q.: *Chem. Soc. Rev.* **2009**, 38, 3242.
49. a) Shimizu H., Onitsuka S., Egami H., Katsuki T.: *J. Am. Chem. Soc.* **2005**, 127, 5396; b) Tanaka H., Nishikawa H., Uchida T., Katsuki T.: *J. Am. Chem. Soc.* **2010**, 132, 12034.
50. Zen J. M., Liou S. L., Kumar A. S., Hsia M. S.: *Angew. Chem. Int. Ed.* **2003**, 42, 577.
51. Hirao T., Shiori J., Okahata N.: *Bull. Chem. Soc. Jpn.* **2004**, 77, 1763.
52. Hasegawa E., Takizawa S., Seida T., Yamaguchi A., Yamaguchi N., Chiba N., Takahashi T., Ikeda H., Akiyama K.: *Tetrahedron* **2006**, 62, 6581.
53. Herance J. R., Ferrer B., Bourdelande J. L., Marquet J., García H.: *Chem. Eur. J.* **2006**, 12, 3890.
54. Osawa M., Nagai H., Akita M.: *Dalton Trans.* **2007**, 827.
55. Nagib D. A., Scott M. E., MacMillan D. W. C.: *J. Am. Chem. Soc.* **2009**, 131, 10875.
56. Shih H.-W., Vander Wal M. N., Grange R. L., MacMillan D. W. C.: *J. Am. Chem. Soc.* **2010**, 132, 13600.
57. Du J., Yoon T. P.: *J. Am. Chem. Soc.* **2009**, 131, 14604.
58. Ischay M. A., Lu X., Yoon T. P.: *J. Am. Chem. Soc.* **2010**, 132, 8572.
59. Lu Z., Shen M., Yoon T. P.: *J. Am. Chem. Soc.* **2011**, 133, 1162.
60. Tucker J. W., Narayanam J. M. R., Krabbe S. W., Stephenson C. R. J.: *Org. Lett.* **2010**, 12, 368.
61. Furst L., Matsuura B. S., Narayanam J. M. R., Tucker J. W., Stephenson C. R. J.: *Org. Lett.* **2010**, 12, 3104.
62. Tucker J. W., Nguyen J. D., Narayanam J. M. R., Krabbe S. W., Stephenson C. R. J.: *Chem. Commun.* **2010**, 46, 4985.
63. Condie A. G., González-Gómez J. C., Stephenson C. R. J.: *J. Am. Chem. Soc.* **2010**, 132, 1464.
64. Dai C., Narayanam J. M. R., Stephenson C. R. J.: *Nature Chem.* **2011**, 3, 140.
65. a) Nguyen J. D., Tucker J. W., Konieczynska M. D., Stephenson C. R. J.: *J. Am. Chem. Soc.* **2011**, 133, 4160; b) Tucker J. W., Narayanam J. M. R., Shah P. S., Stephenson C. R. J.: *Chem. Commun.* **2011**, 47, doi:10.1039/c1cc10827a; For a related photochemical removal of PMB protecting group using flavin photocatalysis, see: c) Lechner R., König B.: *Synthesis* **2010**, 1712.
66. Koike T., Akita M.: *Chem. Lett.* **2009**, 38, 166.
67. Andrews R. S., Becker J. J., Gagné M. R.: *Angew. Chem. Int. Ed.* **2010**, 49, 7274.
68. Rueping M., Vila C., Koenigs R. M., Poschary K., Fabry D. C.: *Chem. Commun.* **2011**, 47, 2360.

69. a) Beeson T. D., Mastracchio A., Hong J. B., Ashton K., MacMillan D. W. C.: *Science* **2007**, 316, 582; b) Jang H. Y., Hong J. B., MacMillan D. W. C.: *J. Am. Chem. Soc.* **2007**, 129, 7004; c) Kim H., MacMillan D. W. C.: *J. Am. Chem. Soc.* **2008**, 130, 398; d) Wilson J. E., Casarez A. D., MacMillan D. W. C.: *J. Am. Chem. Soc.* **2009**, 131, 11332; e) Devery III J. J., Conrad J. C., MacMillan D. W. C., Flowers II R. A.: *Angew. Chem. Int. Ed.* **2010**, 49, 6106; f) Mastracchio A., Warkentin A. A., Walji A. M., MacMillan D. W. C.: *Proc. Natl. Acad. Sci. U.S.A.* **2010**, 107, 20648, and references therein.
70. For recent reports on eosin as photoredox catalyst, see: a) Lee S. H., Nam D. H., Park C. B.: *Adv. Synth. Catal.* **2009**, 351, 2589; b) Lazarides T., McCormick T., Du P., Luo G., Lindley B., Eisenberg R.: *J. Am. Chem. Soc.* **2009**, 131, 9192; c) Labat F., Ciofini I., Hratchian H. P., Frisch M., Raghavachari K., Adamo C.: *J. Am. Chem. Soc.* **2009**, 131, 14290; d) Jhonsi M. A., Kathiravan A., Renganathan R.: *J. Mol. Struct.* **2009**, 921, 279.
71. a) Baik T.-G., Luiz A. L., Wang L.-C., Krische M. J.: *J. Am. Chem. Soc.* **2001**, 123, 6716; b) Wang L.-C., Jang H.-Y., Roh Y., Lynch V., Schultz A. J., Wang X., Krische M. J.: *J. Am. Chem. Soc.* **2002**, 124, 9448; c) Yang J., Cauble D. F., Berro A. J., Bauld N. L., Krische M. J.: *J. Org. Chem.* **2004**, 69, 7979; d) Roh Y., Jang H.-Y., Lynch V., Bauld N. L., Krische M. J.: *Org. Lett.* **2002**, 4, 611; e) Yang J., Felton G. A. N., Bauld N. L., Krische M. J.: *J. Am. Chem. Soc.* **2004**, 126, 1634.
72. For references on radical cation cyclizations, see: a) Bell F. A., Crellin R. A., Fugii N., Ledwith A.: *J. Chem. Soc., Chem. Commun.* **1969**, 251; b) Carruthers R. A., Crellin R. A., Ledwith A.: *J. Chem. Soc., Chem. Commun.* **1969**, 252; For reviews, see: d) Ledwith A.: *Acc. Chem. Res.* **1972**, 5, 133; e) Bauld N. L., Bellville D. J., Harirchian B., Lorenz K. T., Pabon R. A., Jr., Reynolds D. W., Wirth D. D., Chiou H. S., Marsh B. J.: *Acc. Chem. Res.* **1987**, 20, 371; f) Bauld N. L.: *Tetrahedron* **1989**, 45, 5307.
73. a) Giese B., Dupuis J.: *Angew. Chem., Int. Ed. Engl.* **1983**, 22, 622; b) Giese B.: *Angew. Chem., Int. Ed. Engl.* **1989**, 28, 969.
74. Appel R.: *Angew. Chem., Int. Ed. Engl.* **1975**, 14, 801.
75. a) Fancy D. A., Kodadek T.: *Proc. Natl. Acad. Sci. U.S.A.* **1999**, 96, 6020; b) Fancy D. A., Denison C., Kim K., Xie Y., Holdeman T., Amini F., Kodadek T.: *Chem. Biol.* **2000**, 7, 697.
76. Amini F., Denison C., Lin H.-J., Kuo L., Kodadek T.: *Chem. Biol.* **2003**, 10, 1115.
77. Lee J., Yu P., Xiao X., Kodadek T.: *Mol. BioSyst.* **2008**, 4, 59.
78. Lee J., Udugamasooriya D. G., Lim H. S., Kodadek T.: *Nat. Chem. Biol.* **2010**, 6, 258.
79. a) Barton J. K., Olmon E. D., Sontz P. A.: *Coord. Chem. Rev.* **2011**, 255, 619; b) Herman L., Ghosh S., Defrancq E., Kirsch-De Mesmaeker A.: *J. Phys. Org. Chem.* **2008**, 21; c) Szaćiłowski K., Macyk W., Drzewiecka-Matuszek A., Brindell M., Stochel G.: *Chem. Rev.* **2005**, 105, 2647.
80. Elvin C. M., Carr A. G., Huson M. G., Maxwell J. M., Pearson R. D., Vuocolo T., Liyou N. E., Wong D. C. C., Merritt D. J., Dixon N. E.: *Nature* **2005**, 437, 999.
81. Elvin C. M., Brownlee A. G., Huson M. G., Tebb T. A., Kim M., Lyons R. E., Vuocolo T., Liyou N. E., Hughes T. C., Ramshaw J. A. M., Werkmeister J. A.: *Biomaterials* **2009**, 30, 2059.
82. Syedain Z. H., Bjork J., Sando L., Tranquillo R. T.: *Biomaterials* **2009**, 30, 6695.
83. Yu Y., Cui S.: *Langmuir* **2009**, 25, 11272.
84. Yu Y., Zhang H., Zhang C., Cui S.: *Chem. Commun.* **2011**, 47, 929.
85. You X., Zou G., Ye Q., Zhang Q., He P.: *J. Mater. Chem.* **2008**, 18, 4704.

86. Lalevée J., Blanchard N., Tehfe M.-A., Morlet-Savary F., Fouassier J. P.: *Macromolecules* **2010**, *43*, 10191.
87. DeClue M. S., Monnard P. A., Bailey J. A., Maurer S. E., Collis G. E., Ziock H. J., Rasmussen S., Boncella J. M.: *J. Am. Chem. Soc.* **2009**, *131*, 931.
88. Borak J. B., Falvey D. E.: *J. Org. Chem.* **2009**, *74*, 3894.
89. Borak J. B., Lee H. Y., Raghavan S. R., Falvey D. E.: *Chem. Commun.* **2010**, *46*, 8983.
90. For overviews on photochemical strategies to remove protecting groups, see: a) Pelliccioli A. P., Wirz J.: *Photochem. Photobiol. Sci.* **2002**, *1*, 441; b) Bochet C. G.: *J. Chem. Soc., Perkin Trans. 1* **2002**, 125; For related overviews on photochemistry towards manipulating molecules in complex biological systems, see: c) Deiters A.: *ChemBioChem* **2010**, *11*, 47; d) Lee H. M., Larson D. R., Lawrence D. S.: *ACS Chem. Biol.* **2009**, *4*, 409.
91. Flamigni L., Barbieri A., Sabatini C., Ventura B., Barigelletti F.: *Top. Curr. Chem.* **2007**, *281*, 143.
92. For photocatalytic reduction of acetylpyridine to pinacol using *fac*-[Re(bpy)(CO)<sub>3</sub>-(4-(MeCO)py)]SbF<sub>6</sub> catalyst, see: Hori H., Koike K., Takeuchi K., Ishitani O.: *Chem. Lett.* **2000**, 376.
93. For photochemical dehydrogenation of Biginelli compounds by rhenium(I) complexes with visible light and CCl<sub>4</sub>, see: Liu Q., Li Y. N., Zhang H. H., Chen B., Tung C. H., Wu L. Z.: *J. Org. Chem.* **2011**, *76*, 1444.
94. For overview on bimetallic catalysis promoted with visible light, see: Inagaki A., Akita M.: *Coord. Chem. Rev.* **2010**, *254*, 1220.
95. Photosensitization with organic dyes is a rich field. For representative examples, see: refs<sup>2,3,16-18,65c</sup> and Barton D. H. R., Haynes R. K., Leclerc G., Magnus P. D., Menzies I. D.: *J. Chem. Soc., Perkin Trans. 1* **1975**, 2055.
96. For recyclable cross-linked polymers for efficient photocatalysis, see: Xie Z., Wang C., deKrafft K. E., Lin W.: *J. Am. Chem. Soc.* **2011**, *133*, 2056.